The Dissertation Committee for Xiaoxi Ju Certifies that this is the approved version of the following dissertation:

The Role of IL-6 in Inflammatory Aortic Aneurysmal Diseases

Committee:

Allan R. Brasier, M.D., Supervisor

Ronald G. Tilton, Ph.D., Supervisor

Ken Fujise, M.D., Chair

Dianna M. Milewicz, M.D., Ph.D.

Gracie Vargas, Ph.D.

Maki Wakamiya, Ph.D.

Dean, Graduate School

The Role of IL-6 in Inflammatory Aortic Aneurysmal Diseases

by

Xiaoxi Ju, B.S.

Dissertation

Presented to the Faculty of the Graduate School of

The University of Texas Medical Branch

in Partial Fulfillment

of the Requirements

for the Degree of

DOCTOR OF PHILOSOPHY

The University of Texas Medical Branch

June, 2012

Dedication

This is dedicated to my beautiful family,

Hui, Zongwei, Daisi, Jayden, Ling and Yonghao,

for always being by my side and providing endless source of motivation;

to my precious friends for their selfless love and care;

and to my esteemed mentors,

Allan Brasier, MD and Ron Tilton, PhD,

for constant guidance, support, patience and encouragement.

Acknowledgements

First and foremost, I would like to thank my mentors, Allan Brasier, M.D. and Ron Tilton, Ph.D., who provided wonderful training and constant supervision and inspiration. I am deeply grateful for their encouragement, support and guidance throughout my graduate study.

My special thanks go to my supervisory committee members consisting of Dr. Ken Fujise, Dr. Allan Brasier, Dr. Ronald Tilton, Dr. Dianna Milewicz (UTHSC-Houston), Dr. Gracie Vargas and Dr. Maki Wakamiya for constructive criticism of this dissertation, and for their help and support on my projects over the years.

Moreover, I would like to thank my excellent colleagues, Dr. Adrian Recinos, Dr. Sutapa Ray and Dr. Yanhua Zhao, our excellent research associates Hong Sun, Wanda LeJeune and Change Lee, who are always ready to help and teach me various experimental skills.

I would like to especially thank our esteemed Vice Dean of Graduate School, Dr. Dorian Coppenhaver, for always encouraging and helping students as a friend and teacher. I am also grateful for the help from our BMB Graduate Program and the GSBS, our estimable Dean, Dr. Cary Cooper, our program director Dr. Tracy Toliver-Kinsky and the administrative staffs Ms. Laura Teed and JoAlice Whitehurst, on every step of my way.

Finally, my deeply thanks go to my family for their consistent support and encouragement. For my all of my dear family members, I owe them the greatest gratitude and utmost respect.

The Role of IL-6 in Inflammatory Aortic Aneurysmal Diseases

Publication No._____

Xiaoxi Ju, Ph.D.

The University of Texas Medical Branch at Galveston, 2012

Supervisor: Allan R. Brasier

Ronald G. Tilton

Interleukin-6 (IL-6), a member of a superfamily of cardioactive cytokines, has been identified as an independent biomarker of vascular diseases including atherosclerosis and aortic aneurysms. Local vascular IL-6 secretion can be induced by dysregulated angiotensin II (Ang II) signaling, producing leukocyte infiltration that results in life-threatening aortic aneurysms and dissections. Precise mechanisms by which IL-6 signaling induces leukocyte recruitment remain unknown. In this study, we employed two experimental animal models to study the role of IL-6 activation in the development and progression of aortic aneurysms. In an Ang II-treated C57BL/6 mice model, we tested the relationship of IL-6 signaling with Th17-induced inflammation in the formation of Ang II-induced aortic dissections. We found that Ang II infusion induced aortic dissections and CD4+-interleukin 17A (IL-17A)-expressing, Th17 cell

accumulation in C57BL/6 mice. IL-6-deficient mice showed blunted local Th17 activation, macrophage recruitment, and reduced incidence of aortic dissections, suggesting the importance of IL-6 signaling in inducing Th17-mediated aneurysmal progression. We further showed the pathological roles of Th17 lymphocytes by depleting Th17 by IL-17A neutralization or genetic mutation and showed decreased aortic chemokine MCP-1 production and macrophage recruitment, leading to a reduction in aortic dissections. We also established clinical relevance by showing increased Th17 infiltration into the aortic adventitial-medial border in patients with ascending aortic dissections. These findings indicate that IL-6 signaling converges on Th17 recruitment and IL-17A signaling upstream of macrophage recruitment, mediating vascular inflammation and aortic dissections. In another mouse model with spontaneous aortic aneurysms due to Marfan Syndrome (MFS) caused by *Fbn-1* gene mutation (mgR homozygotes), we also reported elevated IL-6 signaling and increased macrophage recruitment in ascending aneurysmal tissues. To study the role of IL-6 signaling, we generated mgR homozygotes with IL-6 deficiency (DKOs), which showed reduction in aneurysmal dilation at late stage of disease with unaffected survival rate. Moreover, we reported that IL-6 deficiency led to decreased ECM degradation that is associated with reduced levels of local MMPs. These findings suggests the activation of IL-6-mediated inflammatory signaling contributed to aneurysmal progression in MFS through recruitment of leukocytes and stimulation of MMP expression, thus aggravating ECM degradation and vascular remodeling.

Table of Contents

List of Tables

List of Figures

Chapter 1

General Introduction

1.1 AORTIC ANEURYSMAL DISEASES

Aortic aneurysms and aortic dissections account for ~16,000 deaths in the United States annually (Kuivaniemi et al., 2008). Recent evidence suggests that enhanced vascular inflammation underlies the progression of both abdominal aortic aneurysms and thoracic aortic aneurysms (Guo et al., 2006a). Common pathologic features of vascular inflammation aneurysmal disease include recruitment and activation of immune cells to the vessel wall, myofibroblast differentiation and extracellular matrix (ECM) remodeling.

1.1.1 Types of aortic aneurysms

Aortic aneurysms are primarily classified based on anatomic locations (Kuivaniemi et al., 2008). Abdominal aortic aneurysms (AAA) primarily develop in the infrarenal segment of the abdominal aorta in humans or suprarenal aorta in rodent models. It predominantly affects elderly males, and is associated with hypertension, vascular inflammation and/or atherosclerosis (Guo et al., 2006a). Initial pathological events in AAA involve recruitment and infiltration of leukocytes into the aortic adventitia and media, which are associated with the production of inflammatory cytokines, chemokine, and reactive oxygen species (ROS). Expression of macrophage activating cytokines is increased both systemically and locally in AAA. Importantly, as a major source of ECM-degrading matrix metalloproteinases (MMPs), recruited activated macrophages promote structural remodeling by degrading elastin and collagen in the vessel wall (Longo et al., 2002). Moreover, in expanding aneurysmal tissues, increased

infiltration of inflammatory cells may amplify MMP production by resident vascular cells (Pearce and Koch, 1996), facilitating aortic inflammation and structural remodeling. In contrast, thoracic aortic aneurysms (TAA) are etiologically separable from AAA due to their strong genetic influence affecting areas including the ascending aorta, aortic arch, and/or descending aorta. Common genetic disorders associated with TAAs include Marfan's Syndrome and Loeys-Dietz syndrome. Recent studies have also identified an inflammatory component in the etiology of TAA (Ejiri et al., 2003). In TAA in patients undergoing surgical repair, enhanced expression of cytokines, such as interleukin-6 (IL-6) and interferon-γ (IFN-γ), as well as enhanced NADPH oxidase and reactive oxygen species (ROS) tone are found in aortic tissues. These events are spatially correlated with increased monocyte/macrophage accumulation and enhanced MMP production. In contrast, thoracic aortic aneurysms (TAA) are etiologically separable from AAA due to their strong genetic influence affecting areas including the ascending aorta, aortic arch, and/or descending aorta. Common genetic disorders associated with TAAs include Marfan's Syndrome and Loeys-Dietz syndrome. Recent studies have also identified an inflammatory component in the etiology of TAA (Ejiri et al., 2003). In TAA in patients undergoing surgical repair, enhanced expression of cytokines, such as interleukin-6 (IL-6) and interferon-γ (IFN-γ), as well as enhanced NADPH oxidase and reactive oxygen species (ROS) tone are found in aortic tissues. These events are spatially correlated with increased monocyte/macrophage accumulation and enhanced MMP production.

1.1.2 Cells and molecules implicated in inflammation in aortic aneurysms

The vascular inflammatory response involves complex interactions between recruited inflammatory cells (lymphocytes, monocytes, macrophages, neutrophils), vascular resident cells [endothelial cells (ECs), vascular smooth muscle cells (VSMCs) and adventitial fibroblasts] and the ECM. The ensuing inflammatory response increases expression of adhesion molecules, growth factors, cytokines and chemokines, which facilitates recruitment and local activation of inflammatory cells and matrix remodeling. Additionally, medial VSMCs and adventitial fibroblasts, as well as immune cells such as macrophages, neutrophils, B- and T- cells, produce cytokines, chemokines, and matrix-degenerating enzymes, facilitating local inflammation and ECM degeneration (Table 1.1).

Cells	Molecules	Roles in Aortic Aneurysms
Fibroblasts	MMP-1	Collagen degradation
	MMP-2	Elastin and collagen degradation
	MCP-1	Monocyte chemotaxis
	IL-6	Macrophage differentiation; MCP-1 induction; systemic acute-phase response
VSMCs	MMP-2	Elastin and collagen degradation
	MMP-13	Collagen degradation

	MT1-MMP	Elastin and collagen degradation; ProMMP-2 activation; facilitate macrophage migration
	MCP-1	Monocyte chemotaxis
	IL-6	Macrophage differentiation; MCP-1 induction; systemic acute-phase response
Macrophages	MMP-3	Elastin and collagen degradation; VEGF activation
	MMP-9	Elastin and collagen degradation; dominant gelatinase in late pathogenesis; TGF-β, VEGF activation; macrophage migration
	MMP-12	Elastin and collagen degradation
	MT1-MMP	Elastin and collagen degradation; ProMMP-2 activation; facilitate macrophage migration
	MIP-1α	T-cell chemotaxis
	IL-8	Neutrophil chemotaxis
	TGF-β	Angiogenesis; MMP induction; Th17 differntiation; myofibroblast differntiation
	IL-6	Macrophage differentiation; MCP-1 induction; systemic inflammatory responses
Th Cells	IFN-γ	Th1 differentiation; macrophage activation
	IL-4	Th2 differentiation; humoral immunity
	IL-17	Macrophage chemotaxis

Table 1.1. Major cell types and molecules involved in vascular inflammatory response in aortic aneurysms.

Recruited CD68-expressing macrophages are found in both the adventitia and intima of aneurysms. They are attracted to the aortic wall by elastin degradation products, CC chemokines [e.g. monocyte chemotactic protein (MCP-1), RANTES, etc] and granulocyte-macrophage colony-stimulating factor (GM-CSF) (Rizas et al., 2009). MCP-1 produced by VSMCs and fibroblasts (Tilson et al., 2000) induces monocyte chemotaxis by binding to CC-chemokine receptor 2 (CCR2). MCP-1 is an important mediator in early pathogenesis of aortic aneurysms because CCR2 deficiency prevents aneurysm formation in various mouse models (Daugherty et al., 2010; Tieu et al., 2009). Additionally, macrophages express 5-lipooxygenase (5-LO), which produces macrophage inflammatory protein 1α (MIP-1α) to recruit T-cells in a paracrine fashion. Locally infiltrated T-cells then magnify the inflammatory cascade by secreting various CC and CXC chemokines, attracting other inflammatory cells to the aneurysmal tissue (Zhao et al., 2004).

CD3+ T-cells are abundant immunomodulatory and pro-inflammatory cells recruited to aneurysmal tissues, accounting for ~50% of local hematopoietic cells (Kuivaniemi et al., 2008). Most T-cell subtypes have been identified, including helper T-cells (Th cells), cytotoxic T-cells and natural killer T-cells (NKT) (Kuivaniemi et al., 2008). Recent studies to identify Th cell subtypes, which are predominant in aneurysms, reported controversial results. Some suggested Th2 was predominant, while other studies suggested Th1 (Galle et al., 2005; Schonbeck et al., 2002).

Aortic resident cells also potentiate inflammation via interactions with recruited immune cells. Adventitial fibroblasts produce cytokines and chemokines such as IL-6,

MCP-1, VEGF, and TNF (Tilson et al., 2000), contributing to leukocytic chemotaxis and activation. Work from our laboratory has found that Ang II stimulates aortic adventitial fibroblasts to recruit monocytes via fibroblast-derived MCP-1, and that the recruited monocytes further promote fibroblast proliferation, adventitial thickening, and additional cytokine production. This fibroblast-monocyte amplification loop may critically mediate adventitial inflammation (Tieu et al., 2010; Tieu et al., 2009).

Many types of enzymes by resident cells and recruited immune cells are of particular interests. For example, MMPs-2, 9 and 12 are capable of inducing ECM degradation (Table 1.1). Collagen degradation in the adventitia can also be caused by MMP-3, 8, and 13, promoting aneurysmal rupture.

Cytokines and chemokines such as IL-8, MIP-1α, and MCP-1 facilitate recruitment and proliferation of inflammatory cells (Table 1.1). Cytokines include TNF, interleukins, interferons, colony stimulating factors, and transforming growth factors, etc. They are produced by diverse cell types including macrophages, T-cells and monocytes, VSMCs and fibroblasts. Circulating cytokines interact with specific receptors on various cell types to activate JAK-STAT, NF-κB, and Smad signaling pathways, regulating expression of various genes controlling inflammatory response involving cell adhesion, permeability and apoptosis. Further, increased local cytokine expression is implicated in aortic aneurysms. Cytokine signaling is also known to increase mitochondrial ROS production, induce integrins to facilitate cellular adhesion and activate MMPs to modify ECM composition.

1.2 IL-6 SIGNALING IN VASCULAR TISSUES

IL-6 is a 26 kDa glycosylated cytokine that acts in a paracrine manner to signal through two distinct mechanisms, termed the classical initiated by membrane receptor binding, and the trans-signaling pathway mediated by soluble IL-6 Rα (Hou et al., 2008). Classical IL-6 signaling is mediated via ligand binding to the IL-6Rα receptor on the cell membrane. The IL-6 trans-signaling pathway, on the other hand, involves binding of soluble IL-6 receptors (sIL-6R) with IL-6 and ubiquitously expressed transmembrane gp130. This process enables IL-6 signaling in cells lacking IL-6Rα.

In IL-6-initiated classical signaling, binding of IL-6 with IL-6Rα causes homodimerization of gp130 expressed on cells, forming an IL-6•IL-Rα•gp130 complex (Boulanger et al., 2003). This induces conformational changes of gp130, which triggers trans-autophosphorylation and activation of Janus tyrosine kinase JAK1. JAK1 in turn induces tyrosine phosphorylation and activation of STAT isoforms STAT1 and STAT3. As transcription factors, they then form homo- and heterodimers with each other, translocate to the nucleus, bind specific DNA sequences and enhance transcription of target genes via interactions with co-factors and co-activators such as p300/CREB-binding protein (CBP) and Positive Transcription Elongation Factor (PTEF-b) (Hou et al., 2008).

IL-6 plays a major role in inducing systemic responses to the presence of vascular inflammation through the hepatic acute-phase response (Brasier et al., 2002). IL-6 has diverse actions in multiple cell types of cardiovascular importance, including ECs, monocytes, platelets, hepatocytes and adipocytes. In the vessel, IL-6 promotes Ang II-

induced ROS production because IL-6 deficiency protects against Ang II-induced endothelial dysfunction (Schrader et al., 2007).

Importantly, a key action of IL-6 is to promote monocyte-to-macrophage differentiation, thus contributing to vascular inflammation. IL-6 stimulation increases esterase and phagocytic activities. It also enhances expression of Fc receptors, macrophage-colony stimulating factor (M-CSF) receptors, the mature macrophages marker F4/80 and other genes important for macrophage differentiation (Hou et al., 2008). Moreover, IL-6 up-regulates MCP-1 expression (Biswas et al., 1998; Tieu et al., 2009) by vascular monocytic cells. MCP-1/CCR2 interactions are important in monocyte recruitment in the development of aneurysms (Boring et al., 1998; Tieu et al., 2009). Also, cell-cell interaction of monocytes and fibroblasts in cocultures induces IL-6 expression and macrophage activation, suggesting a role of IL-6 in monocyte-to-macrophage differentiation (Chomarat et al., 2000; Tieu et al., 2010). Recent studies demonstrated that IL-6-induced downstream gp130-JAK/STAT signaling pathway activation is also important for differentiation of monocytes (Hou et al., 2008).

Current studies indicate that enhanced IL-6 signaling is implicated in vascular inflammation and aneurysm formation. IL-6 is elevated systemically and locally in patients and experimental models of aortic aneurysmal disease. IL-6 deficiency decreases aortic chemokine secretion and macrophage recruitment, and prevents aortic aneurysms and dissections in Ang II-infused mice (Tieu et al., 2009). Conversely, in wild type mice, Ang II infusion potently induces IL-6 expression in the aorta. IL-6 is predominantly expressed by fibroblasts and activated macrophages in the adventitia, instead of by cells

in the media and intima (Recinos et al., 2007). IL-6 signaling pathway is activated in local aortic tissues with Ang II-induced aortic aneurysms (Tieu et al., 2009), where its action promotes monocytic activation and adventitial macrophage accumulation via a chemokine MCP-1-CCR2-based mechanism (Ishibashi et al., 2004; Tieu et al., 2009). These activated macrophages in the vessel wall produce pro-inflammatory cytokines, chemokines, ROS and MMPs, further facilitating local inflammation and remodeling.

Chapter 2

IL-6 mediates aortic inflammation and dissections induced by angiotensin II via the Th17 lymphocyte-IL17 axis in C57BL/6 Mice

(SUBMITTED MANUSCRIPT)

2.1 INTRODUCTION

Angiotensin (Ang) II is the major effector peptide of the renin angiotensin system, whose signaling via the type 1 Ang II receptor induces vascular contractility, hypertrophy and extracellular remodeling (Wi et al., 2009). More recently, Ang II has been shown to induce inflammation, a process mediated by monocyte-macrophage cell recruitment into the adventitial and medial layers of large arteries. Importantly, both human and experimental animal studies have suggested a role for Ang II in the development of aortic aneurysms and dissections (Daugherty et al., 2000).

Vascular inflammation is a stereotypic process producing recruitment of activated leukocytes, monocyte-macrophages and lymphocytes, into all layers of the vascular wall (Daugherty and Cassis, 2002; He et al., 2006). These cells are recruited from the circulation either through the intimal ("inside out") or adventitial ("outside-in") surfaces, through a coordinated process of demargination, tissue infiltration, and local cellular activation (Maiellaro and Taylor, 2007). Of these cell types, cells of the monocyte/macrophage lineage have been shown to mediate the final pathological consequences of vascular inflammation. Ang II-stimulated monocytes are major generators of ROS stress, producers of matrix metalloproteases, and secretors of additional cytokines in the vessel wall (Oya et al., 2011; Rajagopalan et al., 1996; Sprague and Khalil, 2009). These effects result in extracellular matrix degradation, enhanced reactivity to inflammatory agents, endothelial dysfunction, and vascular dilation (Pearce and Shively, 2006). The mechanisms that Ang II-induced cytokines play in this process of local vascular inflammation are not well understood.

IL-6 is the most highly upregulated cytokine in Ang II-stimulated vessels yet identified (Recinos et al., 2007; Tieu et al., 2009), a cytokine identified as an independent biomarker of vascular atherosclerotic risk and for that of aneurysmal rupture (Brown et al., 2003; Zipfel et al., 2003). IL-6 is a member of a superfamily of cardioactive cytokines whose members include cardiotropin, IL-11, and -12, and G-CSF that bind to unique alpha receptors and whose actions are mediated through a common gp130 signal transducer (Mihara et al., 2012). Cellular targets of classical IL-6 signaling include vascular smooth muscle cells, endothelial cells, and monocyte/macrophage populations. Recently, we demonstrated that IL-6 plays a major pathogenic role in aortic aneurysms induced by Ang II because its deficiency significantly blocked monocyte infiltration, reactive oxygen species (ROS) formation, chemotactic cytokine amplification and aortic dissections (Tieu et al., 2009). Although these findings suggest that IL-6 is necessary for macrophage activation in the latter stages of vascular inflammation leading to aortic dissection, IL-6 lacks chemotactic activity and its effects on monocyte recruitment have therefore not been fully explained.

Earlier studies have linked vascular effects of Ang II as mediated by lymphocyte populations (Daugherty et al., 2000; Saraff et al., 2003). Not only are T and B lymphocytes found in Ang II-induced vascular diseases (Ocana et al., 2003), but the effect of Ang II on hypertension, vasomotor dysfunction, oxidative stress, arteriolar thrombosis, and atherosclerosis is prevented with total T-lymphocyte deficiency in mice (Guzik et al., 2007; Senchenkova et al., 2011). These studies suggest that T lymphocytes may play a central role in vascular pathogenesis. More recently, the $CD4^+$ T helper

subset characterized by IL-17A secretion (Th17), a subset distinct from the polarized Th1, Th2, and Treg populations, has been implicated in Ang II-induced atherosclerosis and vascular dysfunction in a hyperlipidemic background (Butcher et al., 2012; Erbel et al., 2009; Madhur et al., 2011; Pietrowski et al., 2011; Smith et al., 2010; van Es et al., 2009). The role of IL-17A/Th17 activation and mechanism for their accumulation in the development and progression of aortic aneurysms and dissections is not known.

In this study, we explored the relationship of IL-6 signaling on formation of the Th17 cell population, and the pathogenic role of IL-17A in the formation of aortic aneurysms and dissections induced by Ang II. Our approach utilized Ang II challenge of normolipidemic (Chan et al., 2012) mouse models with IL-6 and IL-17A deficiencies to assess the rate of aortic dissection. To establish clinical relevance, we also examined Th17 recruitment in human ascending aortic dissections. Our results suggest that a major consequence of vascular IL-6 signaling is on the formation and recruitment of Th17 lymphocytes. Th17, in turn, plays an important role in monocyte recruitment and aortic dissections.

2.2 RESULTS

2.2.1 Establishment of Ang II-induced aortic aneurysms.

We have previously reported that chronic subcutaneous infusion of Ang II at 2,500 ng/kg/min induced aortic aneurysms, defined as dilation of larger than 50% of

normal mice, and dissections, defined as intramural hematoma in the suprarenal aorta (Saraff et al., 2003), in 35-50 % of aged mice (Tieu et al., 2009). In this study, aortic hematomas/dissections were demonstrated with aortic sonography and tissue histochemistry.

In wild-type mice in the C57BL/6 background, histochemical analysis of cross sections in the suprarenal abdominal aorta consistently showed adventitial thickening and blood-filled false lumens located in the tunica adventitia in the Ang II-treated mice. By serial aortic sonography, we observed a moderate 30 % aortic dilatation at the level of suprarenal aorta in all mice after 3-7 days (d), which returned to normal in a subset of animals after 8-14 d. Approximately 40 % of Ang II-infused mice developed areas of focal hemorrhages and development of false lumen, indicating aortic dissection. All mice with dissections maintained an aortic size 50 % greater than control aortas (Figure 2.1).

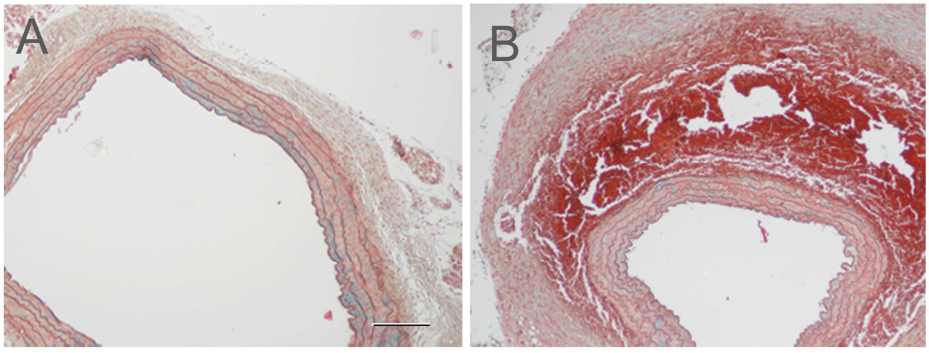

Figure 2.1. Aortic pathology of Ang II infusion in C57BL/6 mice. Ang II-treated mice developed features of aortic remodeling as early as day 3 and continued over the 14-day infusion. As previously demonstrated, moderate early (2-7 days) aortic dilatation of up to 30 % increase in aortic diameter was observed in all mice. Effects of dilation in ~65 % of the Ang II-treated mice (as shown in A) returned to normal level at later stage of infusion (8-14 days). Around 35 % of the Ang II-infused mice developed areas of focal hemorrhages, indicating aortic dissection (as shown in B). Aortic cross

sections in the suprarenal abdominal region clearly showed Ang II–induced adventitial thickening in all animals (A and B) and blood-filled false lumen formation located in the tunica adventitia in 35% of the Ang II-treated mice (B). Scale bar: 50 μM.

2.2.2 IL-6 deficiency reduced aortic dissections induced by Ang II.

To study the role of IL-6 signaling, we treated wild-type and IL-6-deficient mice with Ang II for 14 d and monitor the development of aortic dissections by sonography. We observed a significant lower incidence of formation of aortic dissections (Figures 2.2).

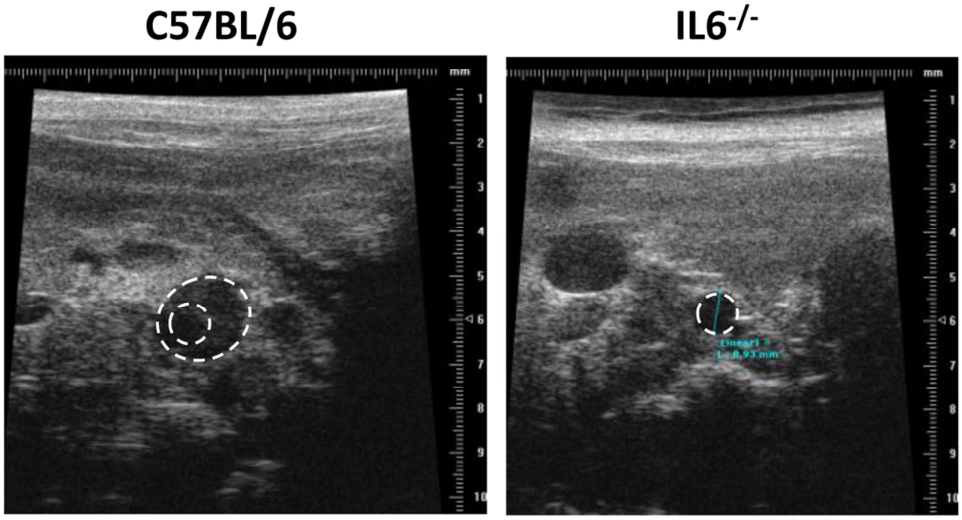

Figure 2.2. Aortic echosonography of suprarenal aortas in Ang II-treated wild-type and IL-6-deficient mice. Age matched C57BL/6 and IL-6 knockout (*Il6*$^{-/-}$) mice were treated with Ang II for 14 d. During Ang II treatment, in vivo imaging of aortas was performed with sonography and diameters of aortas were measured. Representative ultrasound images of Ang II-treated C57BL/6 (n=16) and *Il6*$^{-/-}$ (n=12) mice at d 7 were shown. Dashes in C57BL/6 image represent the true lumen and outer wall of a suprarenal dissection.

Ang II infusions conducted in *Il6*$^{-/-}$ mice in the C57BL/6 background produced a significantly reduced early incidence of aortic dissections after 7 d (31 % in C57BL/6, n=16, vs. 0 % in *Il6*$^{-/-}$, n=12, respectively, 7 d, $p<0.05$), and a trend for reduced dissections after 14 d (Figure 2.3, 38 % in C57BL/6 vs. 8 % in *Il6*$^{-/-}$), without affecting the rate of aortic dilation progression (Figure 2.4).

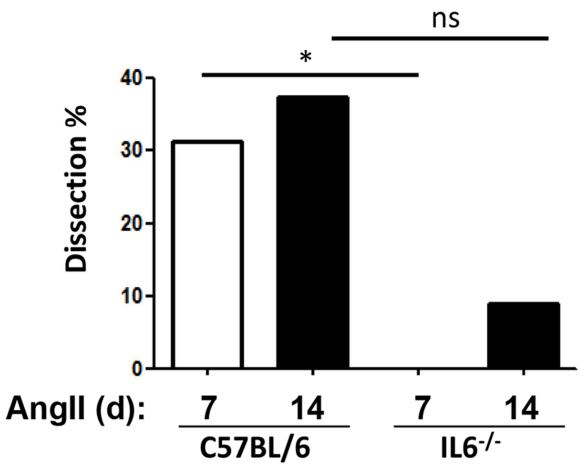

Figure 2.3. Incidence of aortic dissections in Ang II-treated wild-type and IL-6-deficient mice. Percentage of aortic dissection characterized by intramural hematomas is plotted. *, $p<0.05$; ns, not significant.

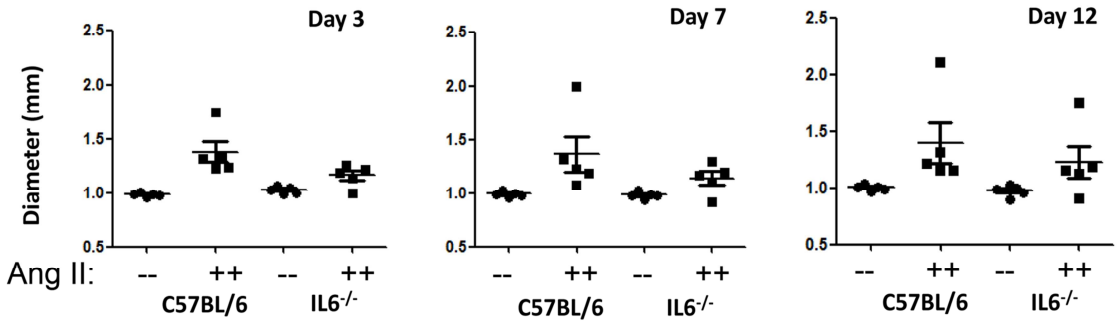

Figure 2.4. Aneurysmal dilation of Ang II-treated wild-type and IL-6-deficient mice. Shown are scatter plots of aortic diameter from the same experiment at 3, 7 and 12 d of Ang II infusion. Circles: sham mice. Squares: Ang II-treated mice.

2.2.3 Ang II induced Th17 recruitment in aortic aneurysmal tissues.

We next tested the mechanism of protection against aortic dissections by IL-6 deficiency. Earlier studies have shown that Ang II induces Th17 recruitment in hyperlipidemic vascular tissues, a cell type mediating hypertension, endothelial dysfunction and atherosclerosis in the *Apoe*$^{-/-}$ background (Erbel et al., 2009; Madhur et al., 2010; Smith et al., 2010).

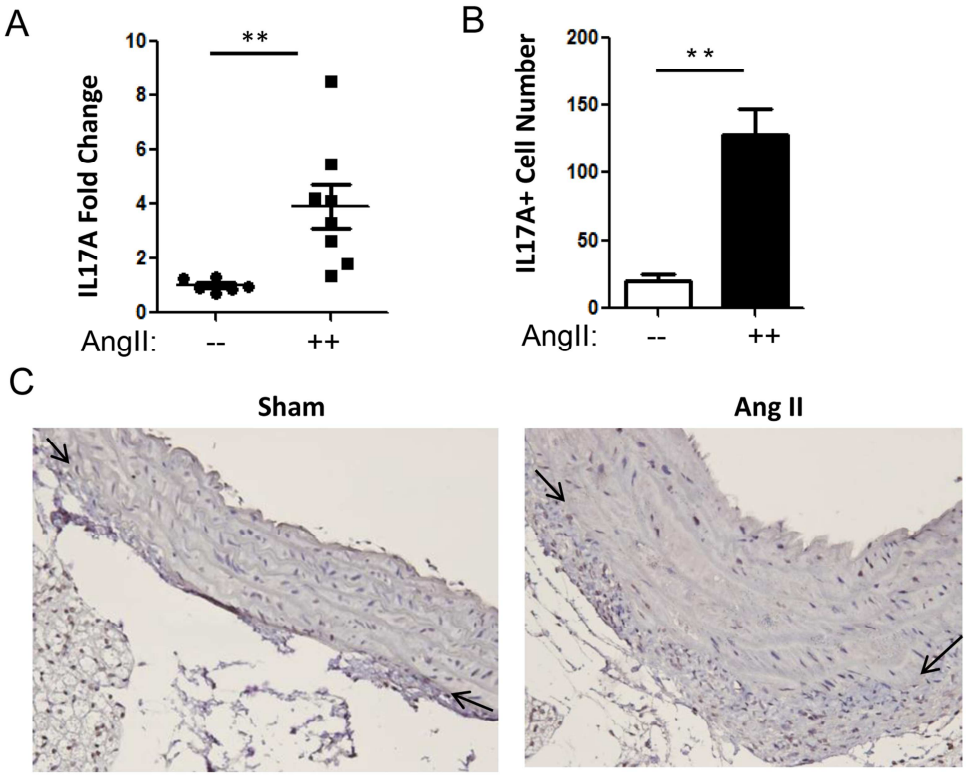

Figure 2.5. Th17 recruitment in aortic aneurysmal tissue in response to Ang II. Sham and Ang II-treated C57BL/6 mice were examined for aortic Th17 recruitment. (A) IL-17A expression was analyzed using Q-RT- PCR. Circles: sham mice. Squares: Ang II-treated mice. (B and C): Aortic sections were stained for IL-17-expressing cells. Cell numbers were quantified microscopically and expressed as cells/visual field under 200X magnification. Arrows indicated border between tunica media and adventitia. **, $p<0.01$. Bottom panel, IHC measurement of IL-17 expression in sham and Ang II

infused aortae. IL-17 staining is increased in the adventitial-medial border (adventitial border is indicated by arrows).

To establish whether Ang II induces Th17 cell recruitment into the aortic wall in normolipidemic mice, we measured the abundance of IL-17A mRNA in the aorta and found it was increased 4-fold relative to sham-infused mice (Figure 2.5, $p<0.01$). We also found that IL-17A-positive staining was observed in both the medial and adventitial layers (Figure 2.5, $p<0.01$), indicating the recruitment of IL-17-expressing Th17 cells in the aneurysmal aortic tissues.

To confirm that Ang II induced the aortic accumulation of the Th17 cell population, we conducted flow cytometric analysis of the dissociated aortae staining for both CD4 and IL-17 (Figure 2.6).

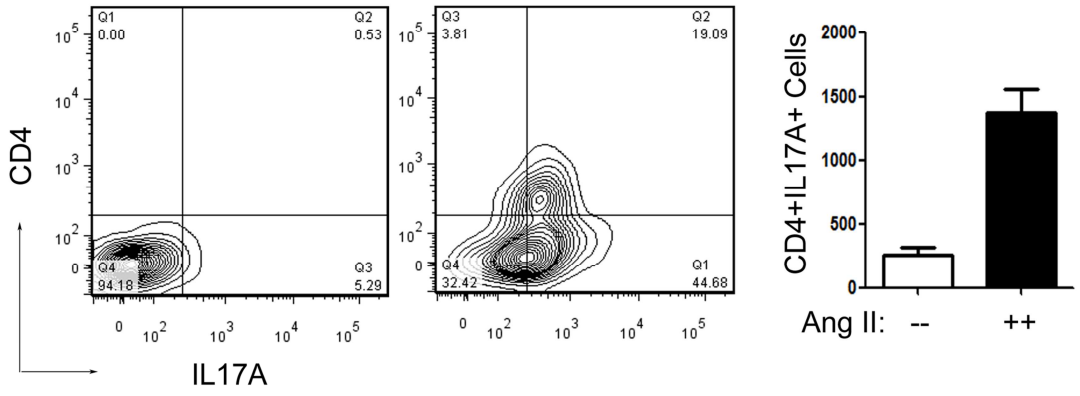

Figure 2.6. Flow cytometry of aortic CD4+IL17A+ cells induced by Ang II. Aged C57BL/6 mice received saline (sham) or high-dose Ang II infusion for 14 d. Flow cytometric analysis of aortic CD4 and IL-17A-positive Th17 cells was performed and numbers of double-positive cells measured. White bars: sham animals treated with saline. Black bars: animals treated with Ang II for 14 d. n=4 in each group.

We treated aged C57BL/6 mice with saline or Ang II for 14 d. It is found that Ang II induced a significant 5-fold recruitment of the CD4+IL17+ Th17 cell population (Figure 2.6, $p<0.01$). The retinoic-acid receptor related orphan receptor (ROR) γ-T, directs Th17 cell differentiation (Oukka, 2008). To further confirm recruitment of Th17 cells, we quantified CD4+RORγT+ cells by flow cytometry. A significant 5-fold increase of CD4+RORγT+ cell numbers (Figure 2.7, $p<0.05$) was also observed in aortic wall in response to Ang II infusion.

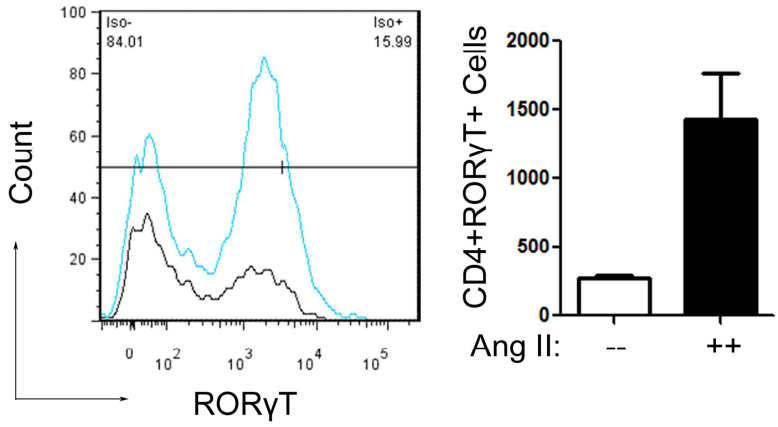

Figure 2.7. Flow cytometric analysis of aortic ROR-γT-expressing cells in CD4+ gating. CD4+ ROR-γT+ cells were stained and quantified. White bars: sham animals treated with saline. Black bars: animals treated with Ang II for 14 d. n=4 in each group.

2.2.4 IL-6 deficiency reduced Ang II-induced macrophage and Th17 recruitment.

We next tested whether local macrophage and T lymphocyte recruitment were affected in the *Il6*$^{-/-}$ background. Flow cytometric staining of aortic CD11b^{+}

macrophages indicated that Ang II-induced macrophage recruitment was abolished in *Il6*$^{-/-}$ mice (Figure 2.8).

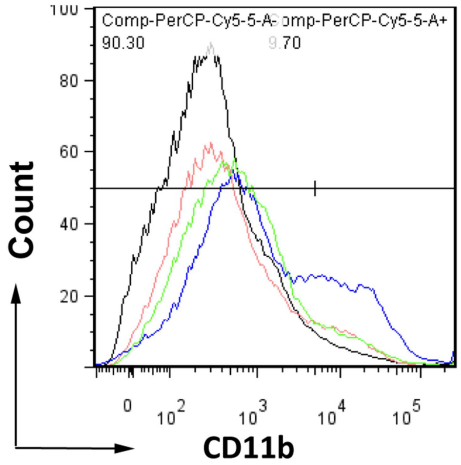

Figure 2.8. Flow cytometry of CD11b+ macrophages in Ang II-treated IL-6-deficient mice. Age matched C57BL/6 and *Il6*$^{-/-}$ mice were treated with Ang II for 14 d. Flow cytometric analysis of CD11b-positive macrophages was performed using aorta-disassociated cells, and numbers of CD11b-positive cells were measured. Black curve: Saline-treated wild-type (WT) C57BL/6. Blue curve: Ang II-treated WT. Red curve: Saline-treated *Il6*$^{-/-}$. Green curve: Ang II-treated *Il6*$^{-/-}$. n=6 for each group.

We next tested if IL-6 deficiency affected expression of IL-17A. A 5-fold increase in aortic wall IL-17A mRNA was produced by Ang II in the *IL-6*$^{+/+}$ genotype; this transcript was decreased in the *Il6*$^{-/-}$ background (Figure 2.9 A; 4.9-fold vs. 2.4-fold vs. sham, $p<0.05$). We also observed that aortic IL-17A$^+$ cells were decreased with IL-6 deficiency by flow cytometry (Figure 2.9 B, 18 % vs. 10 % showing IL-17 staining after gating on CD4$^+$ cells, $p<0.01$). These data indicate that IL-6 deficiency reduces Ang II-induced aortic IL-17A expression and accumulation of Th17 lymphocytes.

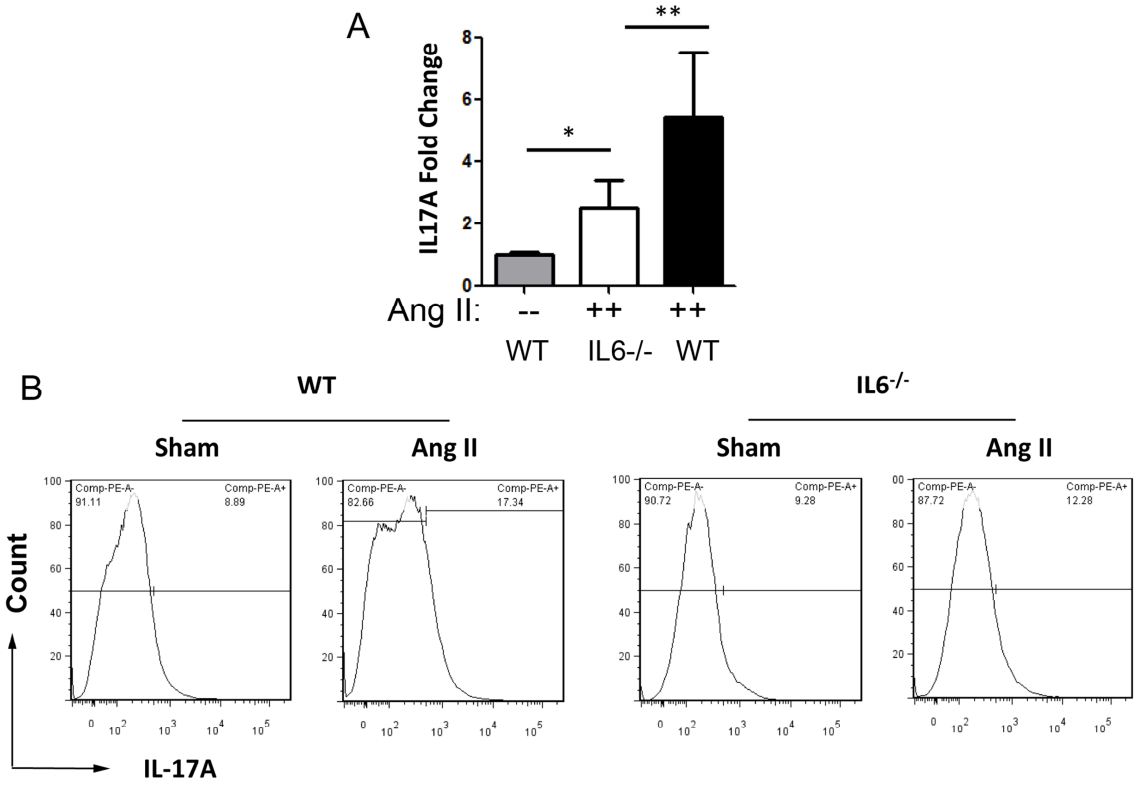

Figure 2.9. IL-6 deficiency decreased Ang II-induced Th17 recruitment in aneurysmal aortic tissue. (A) IL-17A expression was analyzed using quantitative Real-time PCR. Grey bars: Sham-treated C57BL/6. White bars: Ang II-treated *Il6*$^{-/-}$. Black bars: Ang II-treated C57BL/6. n=5. *, $p<0.05$. **, $p<0.01$. (B) Flow cytometric analysis of IL-17A-positive cells in CD4+ gating was performed and numbers of double-positive cells measured. Shown is a histogram of each group (n=6). *Il6*$^{-/-}$ showed abated Th17 recruitment to the aorta.

2.2.5 IL-17A neutralization reduced aortic inflammation and aneurysm formation induced by Ang II.

Since IL-6 plays a pivotal role in Th17 differentiation, we hypothesized that the reduced inflammatory phenotype observed in Ang II-treated *Il6*$^{-/-}$ mice was due, at least in part, to decreased Th17 activation. To test the pathogenic role of IL-17A, we infused

Ang II in mice treated with IL-17A neutralizing antibodies (NAb) or an isotype control antibody (ICAb). First, we confirmed by ELISA that the IL-17A NAb reduced IL-17A secretion from aortic explants in tissue culture (Figure 2.10).

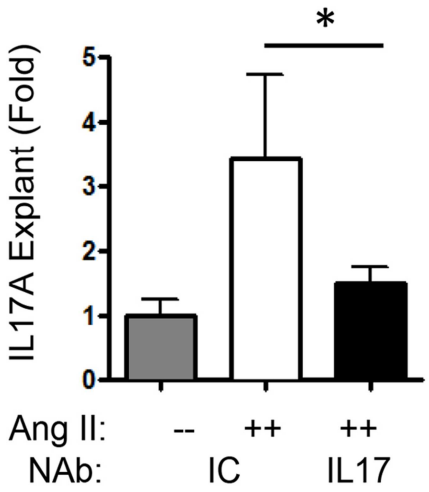

Figure 2.10. IL-17A secretion in aortic explant cultures after IL-17A neutralization. Mice were treated with Ang II and IL-17A NAb or isotype control Ab for 14 d. (A) IL-17A secretion was quantified in aortic explants. Grey bars: Sham. White bars: Ang II and ICAb-treated. Black bars: Ang II and IL-17A NAb-treated. n=4 in each group.

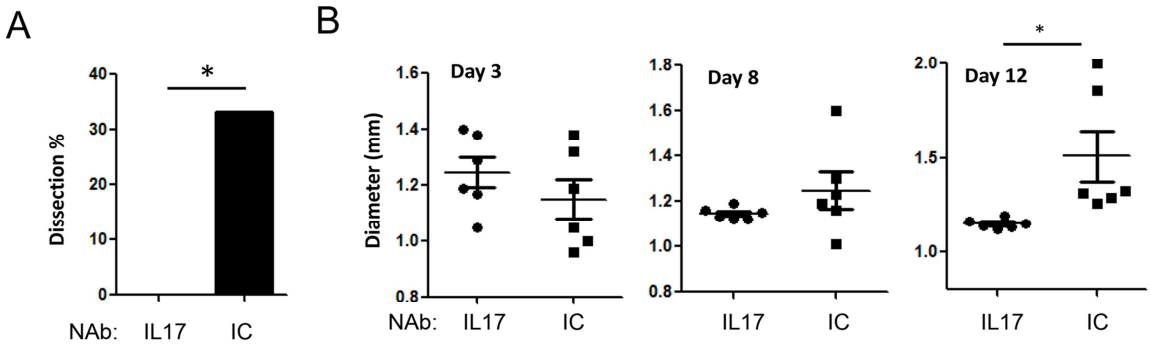

Figure 2.11. Incidence and dilation rate of aortic dissection after IL-17 neutralization. (A) White bars: animals treated with Ang II and IL-17A NAb, n=13. Black bars: animals treated with Ang II and ICAb, n=12. (B) Aortic diameter was quantified at d 3, 8 and 12 for each treatment group. Diameters of aortas were recorded.

Circles: Ang II and and IL-17A NAb-treated mice. Squares: Ang II and ICAb-treated mice.

During Ang II treatment, in vivo imaging of aortas was performed with sonography and diameters of aortas were measured. At 14 d, percentage of aortic dissection featured by presence of intramural hematomas was recorded. We found that a two-week IL-17A NAb treatment significantly reduced Ang II-induced aortic dissections (Figure 2.11 A; 33 % in Ang II plus ICAb, n=12, vs. 0 % in Ang II plus IL-17A NAb, n=13; $p<0.01$). Also, IL-17A neutralization reduced aortic dilation (Figure 2.11 B, $p<0.05$ at d 12) and reduced aortic adventitial thickening.

IL-17A NAb also abolished Ang II-induced aortic Th17 recruitment (Figure 2.12, 12 % in ICAb treatment vs. 4 % with IL-17A NAb treatment, $p<0.05$).

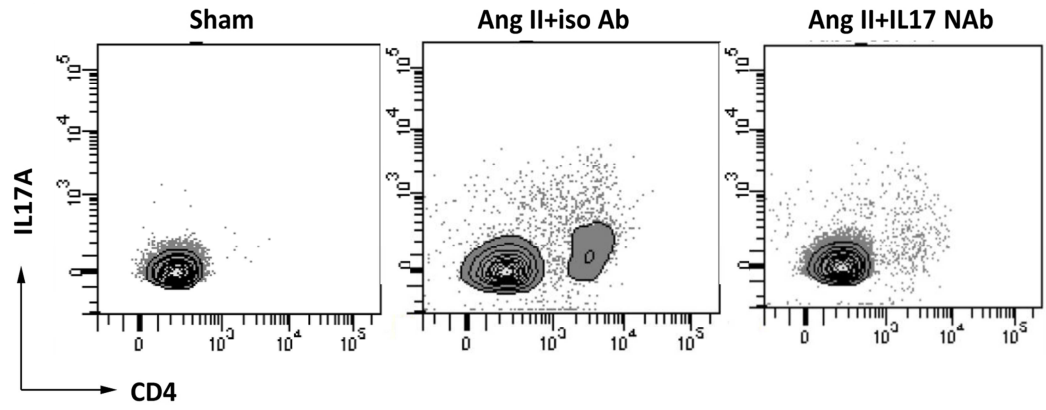

Figure 2.12. Th17 recruitment is abolished in aortas treated with IL-17A NAb. Flow cytometric analysis of aortic CD4 and IL-17A-positive Th17 cells was performed and numbers of double-positive cells measured. n=5.

Neutralization of IL-17A also reduced the aortic macrophage population in the aortic adventitia (Figure 2.13), indicating that IL-17 plays a role upstream of macrophage recruitment in Ang II-induced inflammation.

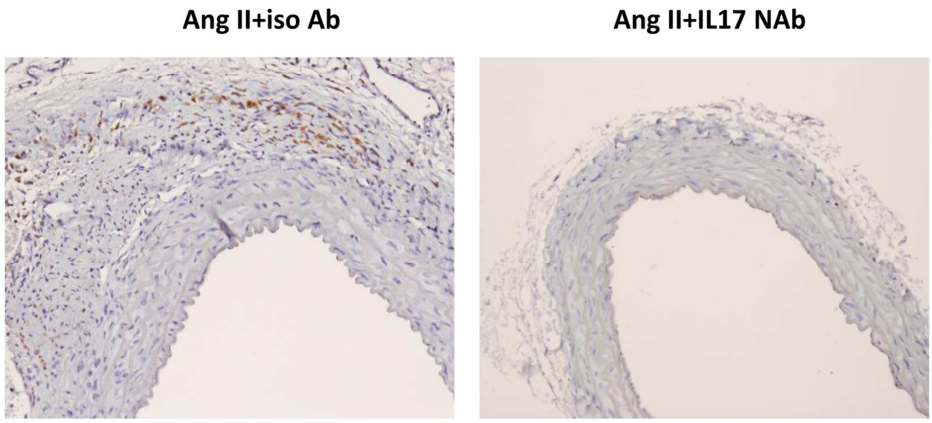

Figure 2.13. IL-17 neutralization led to reduced macrophage infiltration in aortic tissues. Aortic sections were stained for macrophages using MOMA-2 antibodies. Shown is representative of 3 experiments for each treatment group.

2.2.6 IL-17A deficiency blunted inflammatory responses and aortic aneurysm formation.

We next utilized IL-17A-deficient mice to test the role of Th17 lymphocytes in Ang II-induced vascular inflammation and aortic aneurysm formation. We found that, compared with C57BL/6 mice, age-matched *Il17a*$^{-/-}$ mice had a significantly lower incidence of Ang II-induced early (7 d) and late (14 d) aortic dissections (Figure 2.14 A; 41 and 50 % in C57BL/6 vs. 0 and 8 % *Il17a*$^{-/-}$ mice, respectively, n=12, $p<0.05$). In addition, *Il17a*$^{-/-}$ mice developed aortic dissections later (12 d), suggesting that IL-17A plays an early pathogenic role in the formation of aortic dilatation and dissection (Figure

2.14 B, diameters of suprarenal aorta in C57BL/6 and *Il17a*$^{-/-}$ were 1.3 mm vs. 1.0 mm at 6 d, $p<0.05$).

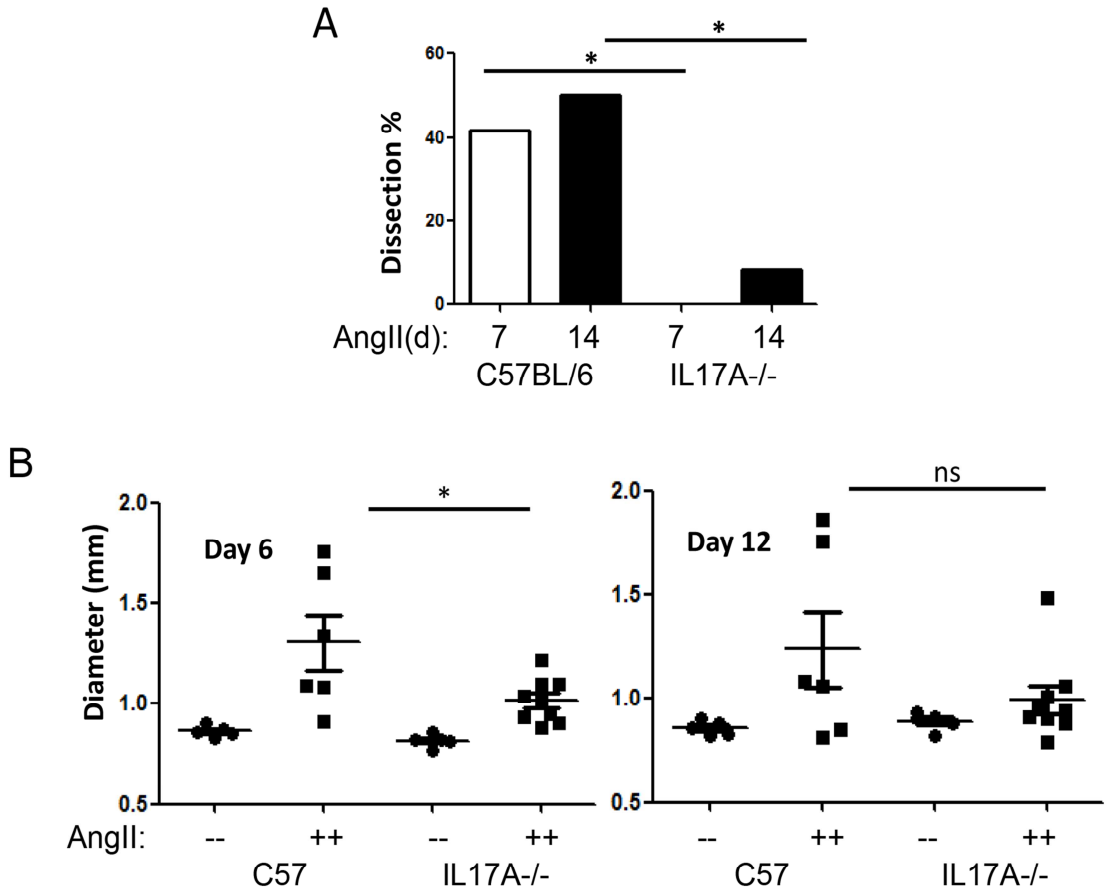

Figure 2.14. IL-17 deficiency reduced incidence and progression rate of Ang II-induced aortic dissections. Age matched C57BL/6 and *Il17a*$^{-/-}$ mice were treated with Ang II for 14 d. During Ang II treatment, *in vivo* imaging of aortas was performed with sonography and diameters of aortas were measured. (A) Percentage of aortic dissection featured by presence of intramural hematomas was recorded (left panel). White bars: animals treated with Ang II for 7 d. Black bars: animals treated with Ang II for 14 d. n=12 in each group. Right panel: diameters of aortas were recorded at 6 and 12 d for each treatment group. Circles: sham mice, n=5 respectively for C57BL/6 and *Il17a*$^{-/-}$. Squares: Ang II-treated mice, n=6 for C57BL/6 and n=9 for *Il17a*$^{-/-}$.

We confirmed the absence of Th17 cells in *Il17a*$^{-/-}$ mice (Figure 2.15, 12 % in C57BL/6 vs. 2 % in *Il17a*$^{-/-}$), suggesting abnormal Th17 homing in these mice may account for protection against aortic aneurysms.

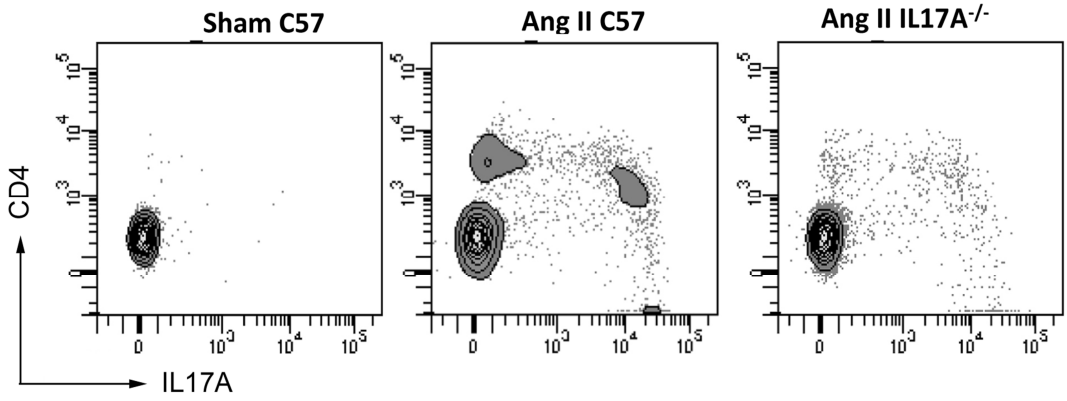

Figure 2.15. Th17 recruitment in aortas is abolished by IL-17A deficiency. Flow cytometric analysis of aortic CD4 and IL-17A+ Th17 cells was performed and numbers of double-positive cells measured. n=4 in each group.

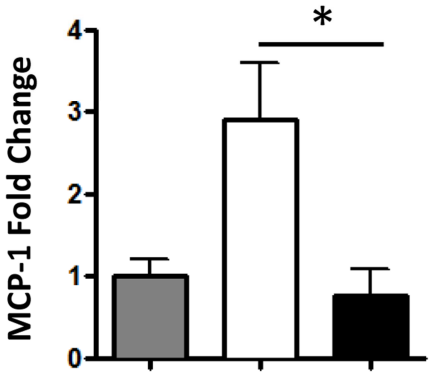

Figure 2.16. MCP-1 secretion from aortic explant culture was reduced by IL-17A deficiency. MCP-1 was measured in aortic explant culture medium. Grey bars: WT-sham; white bars WT-Ang II; black bars *Il17a*$^{-/-}$-Ang II. n=5-6 in each group. *, $p<0.05$.

We further examined cytokine secretion from aortic tissue in response to Ang II treatment. Multi-plex cytokine/chemokine measurements in aortic explant tissue culture media demonstrated that Ang II enhanced expression of MCP-1, which was decreased in the *Il17a*$^{-/-}$ background (Figure 2.16). In addition, aortic macrophage recruitment in response to Ang II was decreased in *Il17a*$^{-/-}$ mice (Figure 2.17; 21 % in C57BL/6 vs. 7 % in *Il17a*$^{-/-}$, $p<0.05$).

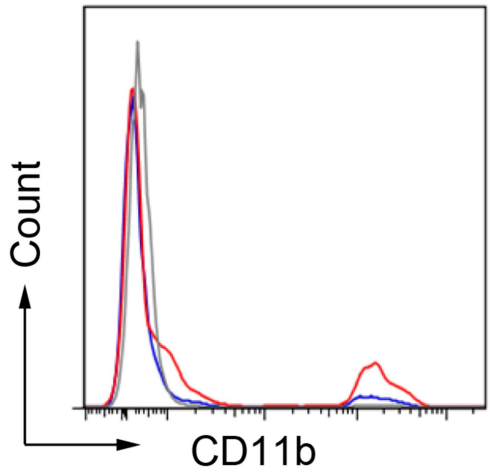

Figure 2.17. CD11b+ macrophage recruitment was blunted in IL-17A-deficient mice. Flow cytometric analysis of CD11b-positive macrophages on aortic disassociated cells was performed. n=4-6 in each group. Grey curves: Sham-treated C57BL/6 at 7 d. Red curves: Ang II-treated C57BL/6 at 7 d. Blue curves: Ang II-treated *Il17a*$^{-/-}$ at 7 d.

2.2.7 Th17 lymphocyte recruitment in patients with thoracic aortic aneurysms.

Previous work has shown that macrophages and T lymphocytes are present in human aortic aneurysms.(He et al., 2006; He et al., 2008) To determine whether aortic Th17 recruitment is increased in human aneurysms, IL-17A expression was quantified

using IHC in thoracic aortic samples from patients with TGF-β receptor mutation (*TGFBR2* R460C). We observed IL-17A staining predominantly at the media-adventitia border (Figure 2.18 A-F). Little IL-17A staining was observed in the medial or intimal layers. Comparing with controls (4 ± 2 cells/field), ascending aortic samples from patients with Type A dissections caused by *TGFBR2* mutation (82 ± 23 cells/field) showed significant enhancement in IL-17A-expressing cell recruitment (Figure 2.18 G, $p<0.01$).

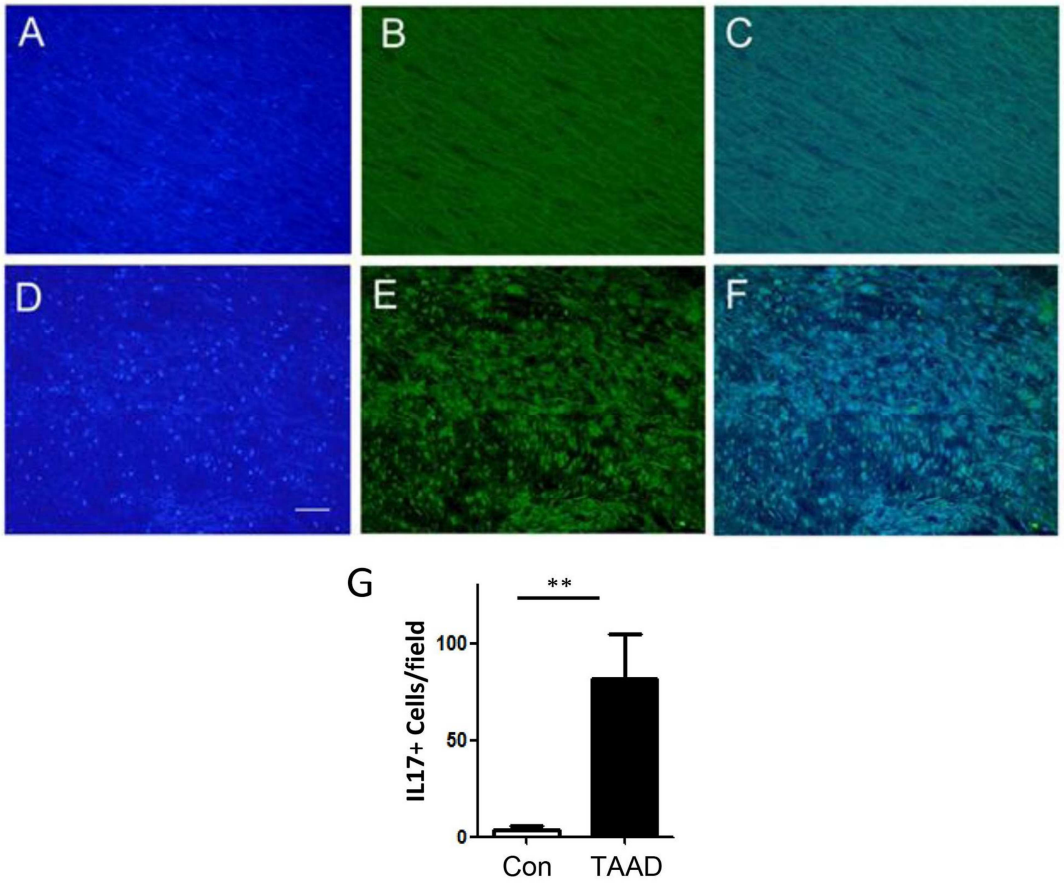

Figure 2.18. Th17 lymphocyte recruitment was found in patients with thoracic aortic aneurysms. In thoracic aortic samples from patients with TGF-β receptor mutation (*TGFBR2* R460C), IL-17A was detected by immunofluorescence microscopy. Positive staining was shown in green (B & E) and conterstained with DAPI

in blue (A &D). Representative images from (A-C) control patients and (D-F) patients with *TGFBR2* mutations were shown. (G) Quantification of IL-17A-positive cells in human aortic samples. White bar: control patient. Black bar: patients with TGHBR2 mutations and Type A dissection. n=3. **, $p<0.01$.

These results extend the pathophysiological relevance of our observations in a mouse model that IL-17-expressing Th17 cells are recruited into the aortic wall, and suggest that these cells may be important contributors to human aortic aneurysms and dissections.

2.3 DISCUSSION

Ang II is a potent inducer of vascular inflammation, IL-6 production and monocyte activation. In this study, we have found that IL-6 converges on the recruitment of Th17 cells, a cell type necessary for the development of Ang II-induced vascular inflammation and aortic aneurysms and dissections by modulating macrophage recruitment. This work extends our previous studies implicating IL-6 signaling with monocyte recruitment, providing a unifying mechanistic pathway where activated macrophage recruitment is coordinated by the $CD4^+$ Th17 lymphocytes. To our knowledge, this is the first application of a genetic deletion of IL-17A in normolipidemic C57BL/6 mice to study the role of IL17A in aortic aneurysms and dissections induced by Ang II.

Lacking direct chemotactic activity, the role of IL-6 in mediating inflammation has been elusive. Previously, we demonstrated that IL-6 signaling in Ang II-stimulated

vascular disease was mediated by macrophage activation, a process involving phospho-Tyr STAT3 formation, loss of F4/80 cell surface staining, and induction of matrix-modifying MMPs (Recinos et al., 2007; Tieu et al., 2009). Interpreted together, these data indicate that IL-6 is locally produced in sufficient concentrations to induce intracellular signaling, and suggest that IL-6 is directly activating monocyte-macrophage differentiation. Our results here are surprising in that they suggest a second major target of activation in the vessel is on the naïve Th0 lymphocyte population, promoting Th17 differentiation. These data suggest that the actions of IL-6 are necessary for Th17 accumulation in the aorta *in vivo*.

Several recent studies have employed hyperlipidemic *ApoE*$^{-/-}$ mice to study the effect of deficiency of total T lymphocytes (Uchida et al., 2010) or Th17 cells (Madhur et al., 2011) in aneurysm formation. Although these previous studies indicated that total T cell or Th17 deficiency was not sufficient to attenuate Ang II-induced aneurysm formation or aneurysmal dilation in *ApoE*$^{-/-}$ mice, our results clearly suggest that defects in Th17 activation protect against early development of aortic dissections by reducing vascular leukocyte infiltration and cytokine/chemokine expression. The different results between these previous studies (Madhur et al., 2011; Uchida et al., 2010) and our current study may be due to the hyperlipidemia caused by *ApoE*$^{-/-}$ background or to differences in the dosage and duration of Ang II challenge.

Th17 cells and IL-17A have been implicated in the pathogenesis of autoimmune and inflammatory diseases (Cheng et al., 2008), and more recently in cardiovascular disease (Eid et al., 2009). Increased circulating Th17 cells and Th17 cell infiltration into

the aorta are found in Ang II-induced hypertension, and IL-17 deficiency blunts these responses and prevents hypertension (Madhur et al., 2010). Further, Th17 cells as well as IL-17 expression in atherosclerosis are increased, and blockade of IL-17A reduced aortic macrophage infiltration, cytokine secretion, and atherosclerotic plaque formation (Smith et al., 2010; Uchida et al., 2010). Interestingly, IL-6 expression is induced by IL-17 and reduced by blockade of IL-17A signaling (Smith et al., 2010), suggesting the proinflammatory effects of IL-6 also could be mediated by Th17 cells. These studies highlight an important proinflammatory role for T cells, especially the Th17 subset, in vascular inflammation.

Monocyte/macrophage recruitment and differentiation are important events in the pathogenesis of inflammatory aneurysms. IL-17 may contribute to inflammatory processes by promoting monocyte chemotasis, adhesion and migration. It has been recently reported that IL-17 induces monocyte migration partially through MCP-1 induction (Shahrara et al., 2009; Shahrara et al., 2010). IL-17A treatment of aorta from atherosclerotic mice promoted aortic CXCL1 expression and monocyte adhesion (Smith et al., 2010). Together, these results highlight an important role of Th17/IL-17 in the pathogenesis of inflammatory aneurysms by promoting cytokine production and monocyte recruitment.

Besides vascular inflammation, hypertension is another well-established pro-pathogenic factor for much cardiovascular morbidity, including aortic aneurysms. Moreover, we and others have previously shown that this dose of Ang II administered subcutaneously by osmotic mini pump results in hypertension in these mouse models.

Our group has also reported that, Ang II infusion at a high dose (2,500 ng/kg/min) produces only modest pressor effects (Tieu et al., 2009). Using a lower dose, 1,000 ng/kg/min, different labs reported that although Ang II produced pronounced increase in arterial blood pressure in other species such as dog or rat, the effects in mice were modest (Daugherty et al., 2000; Daugherty et al., 1991; Hall et al., 1992; Sugiyama et al., 1997). It was also reported that a lower dose of Ang II (1,000ng/kg/min) at this dose, Ang II infusion promoted abdominal aortic aneurysms independent of hypertension in hypercholesterolemic mice since administration of hydralazine lowered systolic blood pressure but did not prevent abdominal aortic aneurysm (AAA) formation or atherosclerosis (Cassis et al., 2009; Daugherty et al., 2000). Moreover, it is noteworthy that recently Madhur et al (Madhur et al., 2010) reported that IL-17A-deficient mice cannot maintain Ang II-induced hypertension comparing with wild-type controls (21-28 d), suggesting that IL-17A did play an important role for the maintenance of late Ang II-induced hypertension. However, at the early stage (1-14 d) which we had examined in this study, there was no significant effect on hypertension in *Il17a*$^{-/-}$ comparing with wild-types.

Our study expands our understanding of the inflammatory process in aneurysm formation by identifying Th17 cells as a central co-ordinator of inflammatory aneurysms. Since IL-17A acts on vascular tissue and induces the production of proinflammatory cytokines and chemokines (Chen et al., 2010b; Erbel et al., 2009; Smith et al., 2010) and ROS (Pietrowski et al., 2011), we hypothesized that IL-17A-expressing Th17 cells may mediate recruitment of leukocytes to sites of inflammation in the aorta. Vascular cells,

including endothelial cells (Chen et al., 2010a), smooth muscle cells (Pietrowski et al., 2011) and monocytes (Butcher et al., 2012) express IL-17RA, the major component of the receptor complex for IL-17A and IL-17F (Gaffen, 2009). Recent *in vitro* and *in vivo* studies suggest an important role of IL-17A in mediating monocyte chemostasis in different systems (Butcher et al., 2012; Shahrara et al., 2009). Rheumatoid arthritis patients treated with IL-17A antibody showed inhibited monocyte chemostasis (Shahrara et al., 2009). $Ldlr^{-/-}$ mice with IL-17R signaling disruption in bone marrow-derived cells resulted in a reduced IL-6 production and attenuated atherosclerosis (van Es et al., 2009). $ApoE^{-/-}$ mice with IL-17RA deficiency demonstrated decreased production of proinflammatory cytokines/chemokine and reduced recruitment of macrophages, T cells, and neutrophils (Butcher et al., 2012). Consistent with these findings, our results indicated that abnormalities in Th17 activation caused by IL-17A deficiency or IL-6 deficiency led to a reduction in macrophage recruitment and cytokine/chemokine expression in the wall of the aorta.

In summary, our data suggest that the Th17 lymphocyte-IL-17 cytokine axis is an important effector arm of Ang II in the genesis of vascular inflammation, and functions upstream of monocyte/macrophage activation. This process is mediated by interplay of the IL-6 in the vascular microenvironment, and that this pathway has direct correlates in human aortic aneurysms.

2.4 Materials and Methods

2.4.1 Animal care and use

All animal experiments were approved by the University of Texas Medical Branch Institutional Animal Care and Use Committee. Mice were housed in the UTMB Animal Resource Center in accordance with the NIH Guidelines for the Care and Use of Animals in Research. Male C57BL/6J wild-type (WT) and *Il6*$^{-/-}$ mice (obtained as breeding pairs and bred in-house; C57BL/6J background) were purchased from Jackson Laboratory (Bar Harbor, Me., USA); IL-17$^{-/-}$ mice were generated as described in Nakae *et al.* (Nakae et al., 2002) and back-crossed into the C57BL/6J background. They were generously provided by David G Harrison, M.D. from Emory University. Mice were maintained on a 12-hour light/dark cycle and were allowed food and water ad libitum. In all experiments, age-matched retired breeders (7 to 10 month-old) were used. For Ang II infusion, anesthetized mice received subcutaneous Alzet osmotic minipumps (Durcet Corp.) delivering either saline (sham) or Ang II (synthesized by the University of Texas Medical Branch peptide synthesis core) at 2,500 ng/kg/min for 10 or 14 days. Ang II-infused mice are treated with 100 µg/mouse i.p. anti-IL-17 (MAB421; R&D Systems) or IgG2A isotype control antibody (MAB006; R&D Systems) at days 0, 4, 8, 12 after starting Ang II infusion.(Erbel et al., 2009; Hofstetter et al., 2005)

2.4.2 Sonoraphy

During Ang II infusion, animals were imaged every 3-5 days with noninvasive sonographic techniques. Serial ultrasound imaging provided visualization of the progression of vessel dilatation and presence of intramural hematomas. Mice were sedated with 1 % inhaled isoflurane (Baxter Healthcare Corporation, Deerfield, IL, USA) delivered via nose cone and were positioned supine and imaged with using Vevo 770 ultrasound machine for small animals (Visualsonics). Abdominal aortas were imaged by two masked investigators in the both transverse and longitudinal axis view with 704 and 707B transducers. Measurements were obtained in triplicate at the level of suprarenal aorta.

2.4.3 Histological Analysis

Ketamine-anesthetized mice were perfused with PBS via the left ventricle to remove blood from tissue. The entire aorta was excised and placed in sterile PBS. Peri-adventitial fat was removed under stereoscope magnification. For histological staining, aortas were fixed in 4 % formalin, dehydrated, and then embedded in paraffin. Aortic tissue was cut at 6 µm serial sections and stained with Movat staining kit (Market Lab Inc) or elastin staining kit (Sigma-Aldrich) according to manufacturers' protocols. Aneurysms were defined as a cross sectional width including the adventitia of the suprarenal aorta that was increased by greater than 50 % compared with aortas from age-matched, saline-infused, control mice. Presence of aortic dissection featured by intramural hematoma was identified under dissecting microscope and was recorded.

Aortic cell numbers and wall thickness were measured on at least 5 random visual fields on sections from 3 different animals under microscope by two masked investigators.

2.4.4 Aortic explant and cytokine analysis

The entire aorta was dissected and immediately placed in 0.5 ml DMEM medium (Cellgro) containing 1× ITS (Sigma-Aldrich) and 0.1 % BSA (Sigma-Aldrich) and incubated in a tissue culture hood at 37° C for 4 hrs. Culture medium was frozen at -80 °C until being assayed for IL-17A and MCP-1 using a multiplex ELISA kit (Lincoplex/Millipore mouse or human adipocyte/cytokine panel) according to the manufacturers' instructions. Cytokine concentrations were determined relative to recombinant standards.

2.4.5 IHC and immunofluorescence

Formalin-fixed, paraffin-embedded sections from suprarenal aortas were rehydrated using serial concentrations of ethanol. When necessary, antigen retrieval was performed with antigen unmasking solution (Vector Laboratories) according to manufacturer's instructions. Sections were blocked using 0.1 % Triton-X, 5 % normal serum of the species producing the secondary antibodies for 1 hr at room temperature. Incubations with primary antibodies were performed at the following concentrations overnight at 4° C: 1:200 rat anti-macrophage (MOMA-2; Abcam), and 1:100 rabbit anti-IL-17A (E-19; Santa Cruz). After washing, secondary antibodies were added at a dilution of 1:500 for 1 hr at room temperature. For immunofluorescence, secondary

antibodies were highly cross-absorbed Alexa Fluor 488–conjugated secondary Ab (Invitrogen), and slides were conterstained with DAPI (Vector Laboratories). For IHC, biotinylated goat anti-rat or anti-rabbit antibodies were used as secondary antibodies, followed by staining with ABC kits per manufacturer's instruction (Vectastain; Vector Laboratories). DAB (Vector Laboratories) was used as substrate and slides were then conterstained with hematoxlin. For human aortic tissue samples, discarded aortic tissue and de-identified clinical data from patients with MFS and TGFBRII mutations were obtained with informed consent under a protocol approved by the University of Texas Health Science Center Institutional Review Board. PFA-fixed, paraffin-embedded sections were taken from the ascending aorta above the sinuses of Valsalva. Sections were stained using a 1:100 dilution of goat anti-IL17A (E-19; Santa Cruz). Secondary antibody-only controls were used to determine staining specificity. Quantitation was performed with the Pro-Image software.

2.4.6 Aortic digestion and flow cytometry

Aortas were dissected, cleaned, minced and placed in 1 ml digestion solution containing 0.6 units/ml Liberase Blendzyme 3 (Roche) and 50 µg/ml porcine pancreatic elastase (Sigma-Aldrich) in a base solution of DMEM. Aortic tissue was digested at 37° C with agitation for 1-2 h. After digestion, cells were filter with 70 µM cell strainer (BD Biosciences) and washed in FACS buffer (0.5 % BSA and 0.02 % NaN3 in DMEM) at 300 g for 5 min. When necessary, red blood cells were removed using RBC lysis solution (Qiagen). For IL-17A staining, cells were digested and incubated in the presence of

PMA (50 ng/mL), ionomycin (1 μmol/L) and brefeldin A (5 μg/mL) for total of 4 hours. For cell membrane antigen staining, murine Fc receptors were blocked using antibodies against mouse CD16/32 antigens (eBioscience) for 10 min on ice. Cells were then incubated with fluorochrome-conjugated primary antibodies anti-CD11b (M1/70; eBiosciences) and anti-CD4 (GK1.5; eBiosciences) for 30-45 min on ice in the dark. Corresponding isotype control antibodies were added at the same concentrations as the antibodies of interest. Cells were then fixed and permeabilized in fixation/permeabilization solution (eBiosciences) for 30 min at 4° C. After washing, cells were stained with fluorochrome-conjugated anti-IL-17A (eBio17B7; eBiosciences) and anti-RORγT (AFKJ5.9; eBiosciences) for 30 min on ice. After incubation, samples were washed 3 times in FACS buffer, centrifuged at 500 g for 5 min, and then fixed in 0.5 % PFA and analyzed by FACSCanto (BD Biosciences). Debris and dead cells, defined by forward scatter, were excluded from analysis. Data were analyzed with FlowJo software.

2.4.7 Quantitative Real-time PCR

Aortas were freshly isolated and frozen in -80° C for later use. Individual frozen aortas were pulverized in liquid nitrogen inside plastic pouches (4.5 mils thick; Kapak SealPAK), resuspended in TriReagent (Sigma-Aldrich), and further homogenized on ice in glass dounce homogenizers (Wheaton). RNA was extracted according to the manufacturer's instructions of TriReagent. RNA then was quantified by Nanodrop (Thermo Scientific) and samples were included when the 260/ 280 nm ratio was >1.6.

Five μg RNA was reverse transcribed using Superscript III (Invitrogen) according to provided directions. Real-time PCR reactions were performed in triplicate using 1 μl of resulting cDNA per 20 μl reaction volume containing iQ SYBR Green Supermix (Bio-Rad). The housekeeping gene GAPDH was used as control. Primers were purchased from SABioscience for the following RNAs: mouse ccl2 (PPM03151F), mouse il17a (PPM03023A). PCR was performed on the CFX96 system (Bio-Rad) according to preset protocol. mRNA was analyzed by the ΔΔCt method.

2.4.8 Data analysis

Data are reported as ± SEM. Differences between 2 groups were analyzed by Student's t test (2-tail, assuming unequal variances). One-way ANOVA was performed when comparing multiple groups, followed by Tukey's post-hoc test to determine significance. Fisher's exact test was performed on the data for aortic dissections to determine significance at different time points because of small group size. In all cases, $p < 0.05$ was considered significant.

Chapter 3

IL-6 regulates vascular inflammation and MMP-mediated ECM degradation in aortic aneurysms in Fbn-1 mutant mice

(SUBMITTED MANUSCRIPT)

3.1 INTRODUCTION

Marfan Syndrome (MFS), an inherited autosomal dominant disorder with high motility rate, affects connective tissues in the skeletal, ocular, respiratory and the cardiovascular systems (Dietz et al., 2005). The most serious complication in patients with MFS is degenerative aortic lesions including progressive aneurysmal dilatation of the thoracic aorta (TAA) and sudden rupture, aortic dissection. Therefore, the most important clinical target for improving survival is to delay or prevent aortic dilatation and dissection by surgical treatment or medical interventions (Williams et al., 2008). Features of TAAs in MFS includes significant pathological remodeling of extracellular matrix (ECM) in the tunica media and adventitia, smooth muscle cell apoptosis, and decreased arterial distensibility (Dietz et al., 2005; Hirata et al., 1991). Recent studies have identified causal relationships between MFS and genetic mutations in fibrillin-1 gene (*FBN-1*) on chromosome 15, which encodes for an important glycoprotein of microfibrils in ECM (Dietz et al., 2005; Dietz and Pyeritz, 1995), or transforming growth factor β receptor 2 (*TGFBR2*) gene on chromosome 3, which encodes for a key mediator of transforming growth factor β (TGF-β) signaling (Mizuguchi et al., 2004). In both cases, abnormally upregulated TGF-β signaling is found to be a critical underlying biochemical event in TAA pathogenesis in MFS. In FBN-1 mutations, insufficient production of fibrillin-1 leads to unstableness of microfibrils and loss-of-sequestering of TGF-β, resulting in over-activation of TGF-β signaling (Kaartinen and Warburton, 2003).

Recently, enhanced Angiotensin II (Ang II) signaling has also been implicated in MFS (Nagashima et al., 2001). Ang II antagonism, including angiotensin receptor

blocker (ARB) losartan and ACE inhibitor perindopril, are reported to be effective to normalize TGF-β levels and TGF-β non-canonical signaling, reduce aortic MMP expression, and prevent aortic dilation in patients with MFS (Carvajal et al., 2008; Habashi et al., 2006; Xiong et al., 2012; Yang et al., 2010). As a vasopressor and a potent inducer of vascular inflammation, Ang II stimulates cytokine, chemokine and reactive oxygen species (ROS) production in endothelial cells (ECs), vascular smooth muscle cells (VSCMs), and fibroblasts, events involved in the pathogenesis of aortic aneurysms (Ejiri et al., 2003; Longo et al., 2002). In VSMCs and adventitial fibroblasts, a major target of Ang II-induced NF-κB signaling is to activate expression of interleukin-6 (IL-6) (Chen et al., 2001; Han et al., 1999). IL-6 is an inflammatory cytokine implicated in many cardiovascular conditions that signals via activation of Janus kinase (JAK) and signal transducer and activator and transcription 3 (STAT3) (Brasier, 2010). Recent studies indicate that enhanced IL-6 signaling is associated with aneurysm development. IL-6 is elevated systemically and locally in patients and experimental models of abdominal aortic aneurysmal (AAAs) disease (Dawson et al., 2006; Dawson et al., 2007; Jones et al., 2001; Tieu et al., 2009). IL-6 signaling pathway was locally activated in Ang II-induced aortic aneurysms (Tieu et al., 2009), where its action promotes aortic monocyte recruitment and monocyte-to-macrophage activation via a chemokine monocyte chemotactic protein-1 (MCP-1)-based mechanism (Biswas et al., 1998; Boring et al., 1998; Ishibashi et al., 2004; Tieu et al., 2009). These activated macrophages in the vessel wall produce pro-inflammatory cytokines, chemokines, ROS

and matrix metalloproteinases (MMPs), further facilitating local inflammation and remodeling.

Although TAA is considered to be a less inflammatory form of aneurysms as comparing with AAA, local inflammatory events are reported in patients and mouse models with MFS (He et al., 2006; He et al., 2008; Pereira et al., 1999; Radonic et al., 2012). In a hypomorphic fibrillin-1 mutant mouse model (mgR/mgR homozygotes), an inflammatory-fibroproliferative response has been described in TAA formation (Pereira et al., 1999). Homozygous mgR mice die between 3 and 6 months of age of dissecting TAAs, and adventitial inflammation may accelerate pathogenesis by stimulating unregulated degradation of elastic matrix. In this mouse model, enhanced monocyte/macrophage infiltration is also pronounced at late stages of disease progression (Pereira et al., 1999). Additionally, aortas from these mice secrete a GxxPG-containing fibrillin-1 fragment to induce macrophage chemotaxis (Guo et al., 2006b) and expression of MMP, which further amplifies matrix degenerated product-mediated chemotaxis (Booms et al., 2006; Booms et al., 2005). Together, these findings suggest that inflammation may participate in extracellular matrix degradation associated with fibrillin deficiency-induced TAAs. However, whether the inflammatory cytokine IL-6 is involved in the pathogenesis of TAAs is not known.

Besides Ang II antagonists, MMP inhibitors, especially doxycycline, are also found to be effective in improving survival in MFS (Habashi et al., 2006; Xiong et al., 2012; Yang et al., 2010). Matrix-degrading MMPs are elevated in aortic tissue in patients with MFS, and are associated with destruction of matrix structural

macromolecules such as elastin and collagen (Biswas et al., 1998; Ikonomidis et al., 2006; Segura et al., 1998). Of numerous MMPs, MMP-2 and MMP-9 expressions are correlated with the stage of aneurysmal dilation (Petersen et al., 2002). They are not only capable of degrading elastin and collagen in the aortic wall, but also able to catalyze activation of TGF-β, further contributing to pathogenesis (Ge and Greenspan, 2006; Wang et al., 2006). Treatment with doxycycline reduces aortic activation of MMP-2 and MMP-9, thus delaying aneurysmal dilatation in MFS (Chung et al., 2008; Xiong et al., 2008). Interestingly, in other disease models, expression of MMP-2 and MMP-9 correlates with IL-6 signaling (Kossakowska et al., 1999; Kusano et al., 1998; Pajulo et al., 1999; Xie et al., 2004). IL-6 stimulates mRNA expression and biological activities of MMP-2 and MMP-9 through soluble IL-6 receptor (sIL-6R) in bone resorption and cancer models (Kossakowska et al., 1999; Kusano et al., 1998). Additionally, high activity of STAT3, the IL-6 downstream signaling protein, is correlated with enhanced MMP activity and blockade of STAT3 or with JAK inhibitors significantly decrease MMP activity (Xie et al., 2004). However, whether IL-6 participates in modulating MMP activity in aneurysm development is unclear.

In this study, we tested the role IL-6 in the pathogenesis of TAA in the mgR/mgR homozygous mouse model of MFS. Using novel imaging techniques, we examined the structural and cellular components of the aortic wall. We investigated the presence of local aortic inflammatory events. We found that expression and secretion of the cytokine IL-6 and the chemokine MCP-1 were both significantly increased in mgR homozygous mice with MFS as comparing with wild-type littermates. The localization of IL-6 and

MCP-1 production was found in the media and adventitia. Recruited by locally secreted cytokines, the infiltration of macrophages was also prominent in the mgR homozygotes. IL-6 deficiency in mgR/mgR mice delayed progression of ascending aorta dilation at late stage without affecting the survival rate. In addition, IL-6 deficiency reduced elastolytic events, decreased recruitment of inflammatory cells, and resulted in better preservation of elastin and collagen contents in ascending aortic wall. Finally, we showed that IL-6 deficiency led to decreases in MMP-2 and MMP-9 activities, suggesting a mechanism in which IL-6 regulated TAA development in MFS by modulating MMP expression and leukocyte recruitment in the aortic wall.

3.2 RESULTS

3.2.1 Characterization of mgR/mgR moude model of MFS.

As previously reported (Pereira et al., 1999), mgR/mgR homozygous *Fbn-1* mutants developed spontaneous thoracic aortic aneurysms at 0-3 month of age and dead of aortic rupture before 6 month (Figure 3.1). We performed transthoracic echosonography to evaluate the establishment and measure the sizes of TAAs. Aortic diameters of wild-type (+/+) and mgR/mgR mutants were measured *in vivo* at 12 weeks (wk) of age at the levels of ascending aorta, supra-aortic ridge and sinus of Valsalva (Figure 3.2).

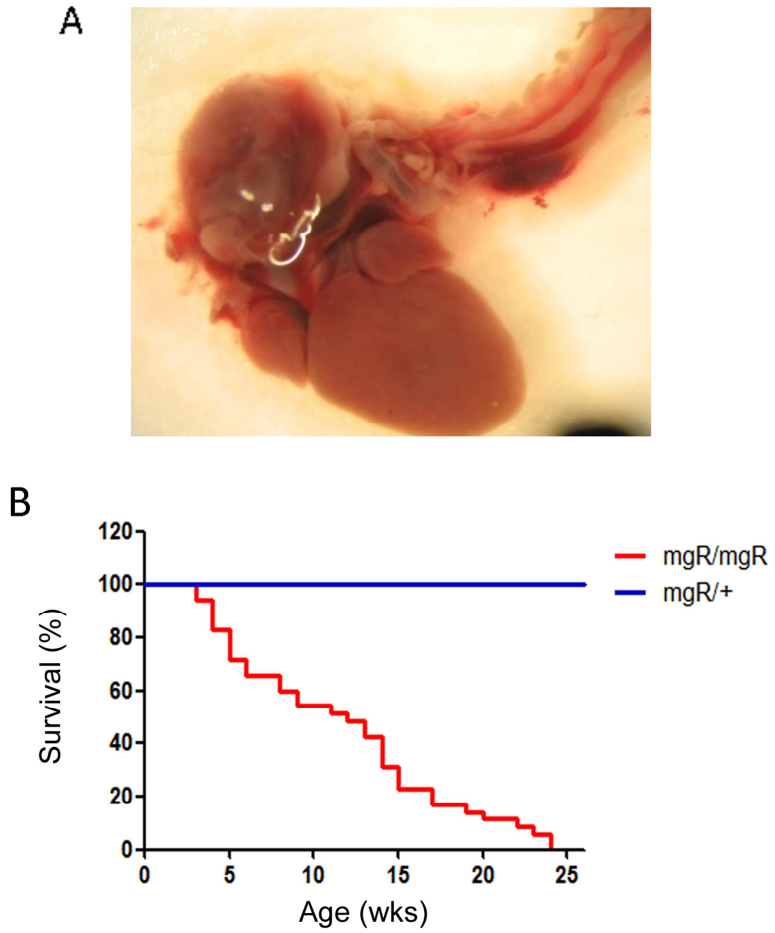

Figure 3.1. mgR homozygotes develop spontaneous TAAs. (A) Representative anatomical image of a TAA formation in a 12 wk-old mgR homozygote. mgR/mgR mice developed spontaneous TAAD that ruptured prematurely. Arrow: TAA in ascending aorta. (B) Survival curves of mgR homozygotes and heterozygotes.

Of these three regions we examined, differences between +/+ and mgR/mgR littermates were only significant at the level of the ascending aorta (Figure 3.3). We therefore chose the ascending aorta in following investigations.

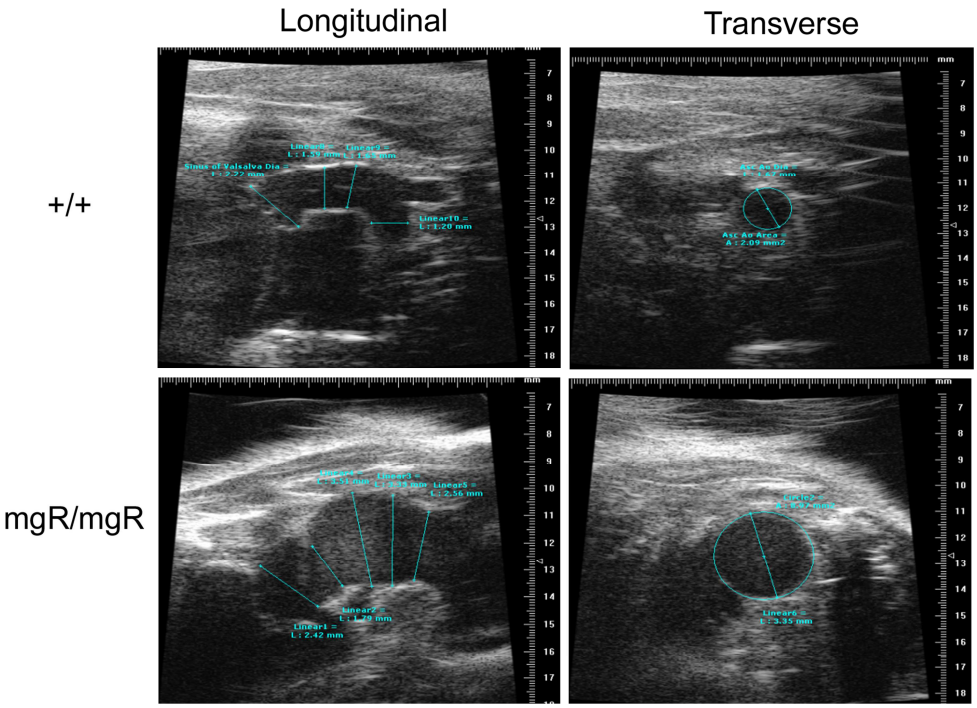

Figure 3.2. Representative echosonography images of the aortic arch in age-matched +/+ and mgR/mgR littermates. Age matched mgR homozygotes, heterozygotes, and wild-type littermates were indentified by genotyping and used for echosonography imaging the throracic aorta at the levels of the ascending aorta (Asc Ao), the supra-aortic ridge (Supra Ao Ridge) and the sinus of valsalva.

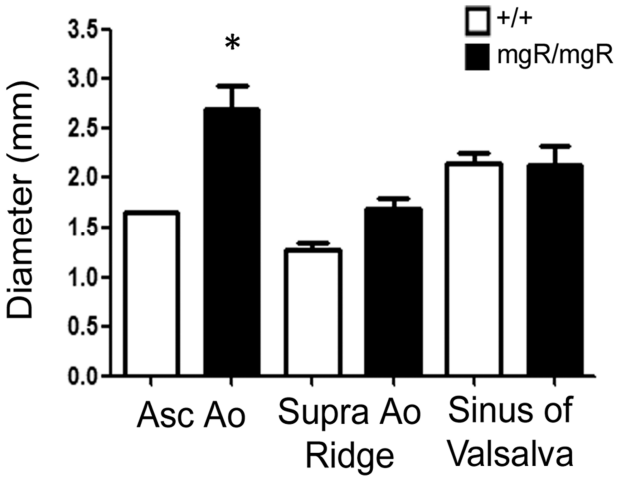

Figure 3.3. Aortic dilatation is significantly increased at the level of ascending aorta in mgR homozygotes. Diameters of thoracic aortas in mgR homozygotes (n=9) and wild-type littermates (n=8) were measured in vivo at the levels of ascending aorta, supra-aortic ridge and the sinus of valsalva. *, $p<0.05$.

Using histological staining in mgR mutants, we observed extensive loss of elastin in the media at this age, exhibiting both breaking and thinning of elastin fibers (Figure 3.4).

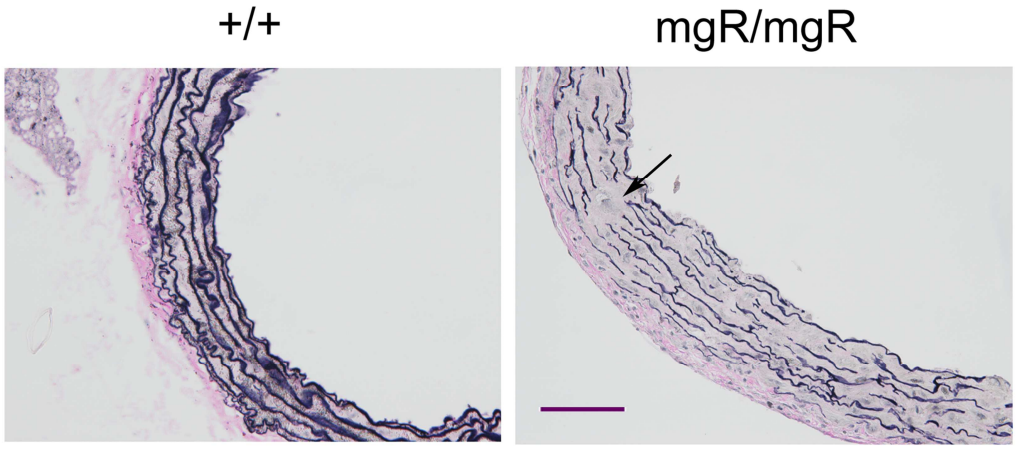

Figure 3.4. Elastin degradation is evident in ascending aortas of mgR homozygotes. Histological staining of elastin (shown in purple), collagen (shown in pink) and SMCs (shown in yellow) in sections of ascending aorta. n=6, respectively. Arrow: breaks in elastin fibers.

We confirmed the degree of elastolysis by multiphoton autofluorescence microscopy (MPA). In wild-type controls, elastin proteins formed smooth sheets in the aortic media, whereas in the mgR mutants, large numbers of holes as large as 50 μM were evident, suggesting substantial elastin degeneration (Top panel, Figure 3.5).

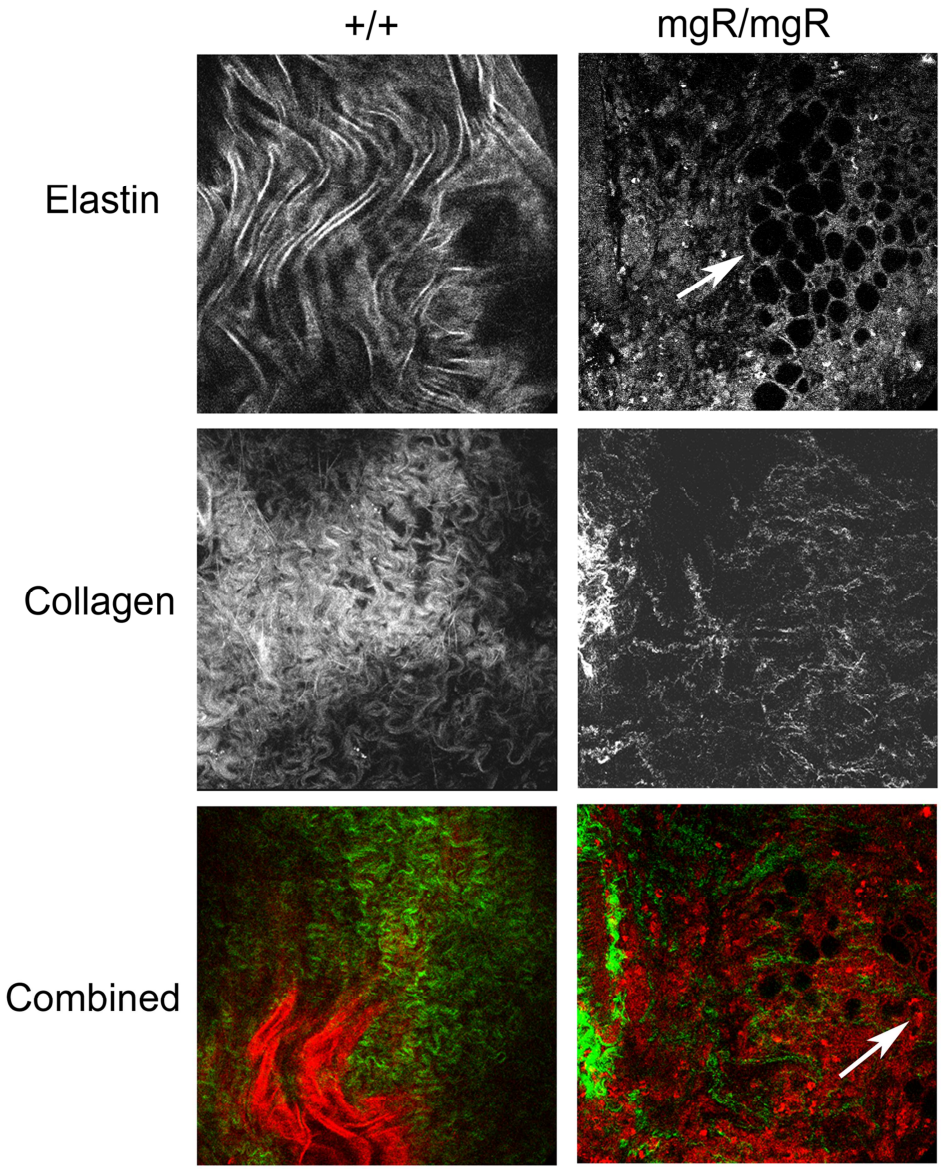

Figure 3.5. SHG and MPA microscopic images of wild-type mice and age-matched aneurysmal mgR/mgR mice. Top panel: Elastin sheets. Middle panel: Collagen fibers in the aortic adventitia. Bottom panel: Combined images of collagen and elastin at the adventitia-media border. Collagen was shown in green and elastin was shown in red. Arrows: Gaps were formed in elastin layers. Cell infiltration is also pronounced at the adventitia-media border. Shown is representative of 3 experiments for each group (n=4-6 in each group). Images were taken in 320X320 μM.

To study the complete structural components of the ascending aortic wall, we also combined MPA and second harmonic generation (SHG) microscopy, which is used to detect collagen contents in different animal models,(Kouchoukos et al., 2006; Pajulo et al., 1999) for imaging of ex vivo aortic samples. SHG images showed that comparing with dense, curly and thick collagen fibers in wild-types, the mgR mutants maintained relatively straightened, dispersed and thin collagen fibers (Middle panel, Figure 3.5), indicating a dramatic loss of collagen content in the adventitia. Moreover, we observed a large number of autofluorescent infiltrating leukocytes in the border between media and adventitia (Bottom panel, Figure 3.5), suggesting immune cell recruitment to the ascending aortic wall at this age.

3.2.2 Expressions of IL-6 and MCP-1 are elevated in mgR/mgR mice with MFS.

In order to study inflammatory processes and identified the involvement of IL-6 signaling in the development of TAA in MFS, we evaluate the expression and secretion of cytokines in the ascending aortas.

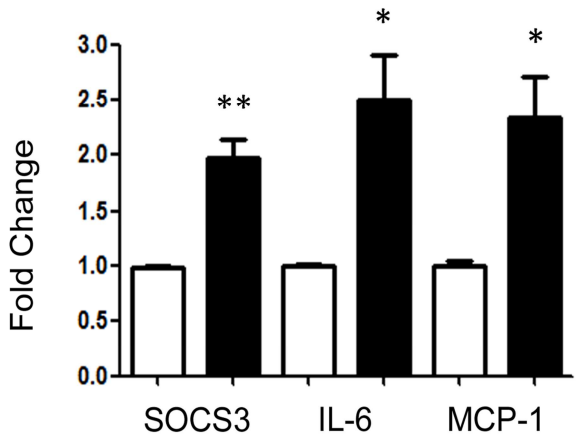

Figure 3.6. IL-6 expression and IL-6 signaling were activated in ascending aortas of mgR homozygotes. Real-time quantitative analysis showed that gene expression levels of IL-6, MCP-1, and IL-6 downstream signaling molecule SOCS3 are significantly elevated, suggesting activation of IL-6 signaling in mgR mutants. *, $p<0.05$. **, $p<0.01$.

We observed a significant 2.4-fold increase in IL-6 expression ($p<0.05$), as well as an increase in the IL-6 downstream target suppressor of cytokine signaling 3 (SOCS3, $p<0.01$), suggesting the activation of IL-6 signaling in mgR/mgR ascending aortas (Figure 3.6). Additionally, expression of MCP-1, an important IL-6 downstream effector and recruiter of macrophages, also elevated relative to wild-type littermates (Figure 3.6, $p<0.05$). We confirmed by ascending aortic explant culture that the local secretion of IL-6, MCP-1 and granulocyte-macrophage colony-stimulating factor (GM-CSF) were enhanced by 2-3 folds (Figure 3.7, $p<0.05$).

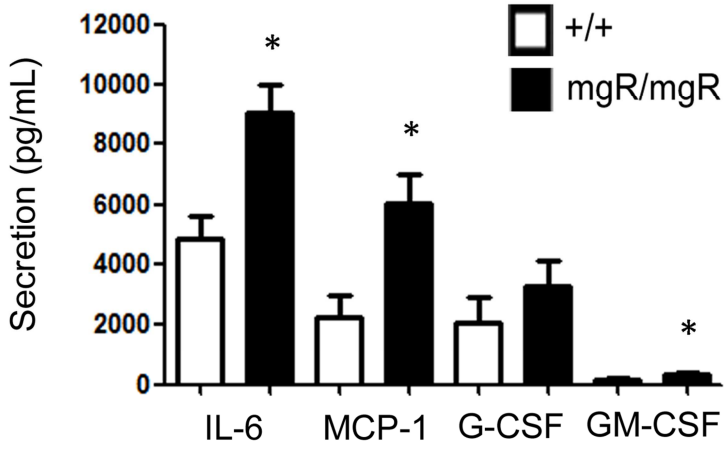

Figure 3.7. Secretion of IL-6, MCP-1 and GM-CSF were increased in mgR homozygotes. Local cytokine and chemokine secretion from thoracic aortic tissues in explant culture medium was measured by multi-plex ELISA. *, $p<0.05$.

IHC staining of ascending aortic sections showed that IL-6 and MCP-1 expressions were mainly localized in the aortic media (Figure 3.8).

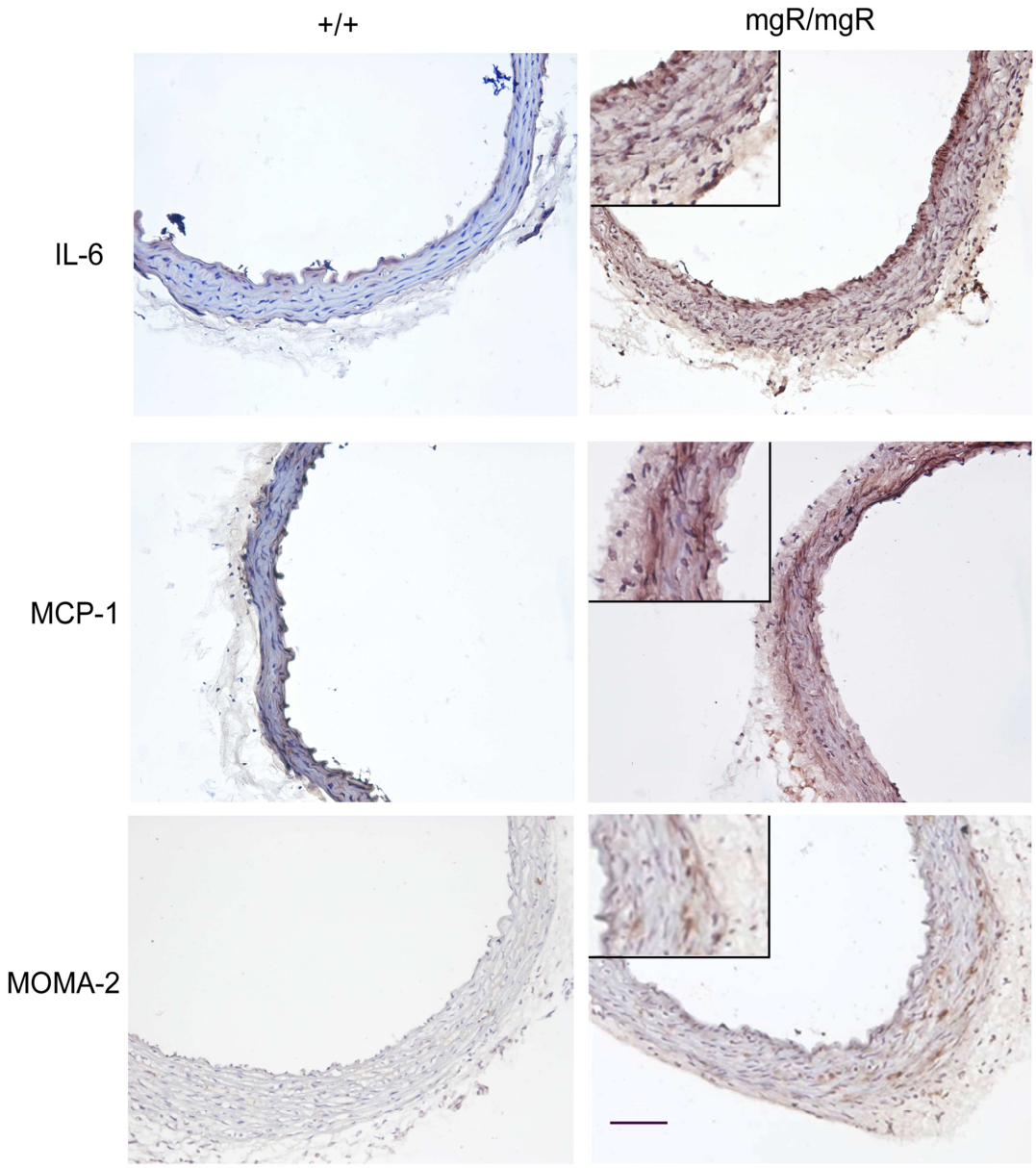

Figure 3.8. IHC staining of IL-6, MCP-1 and the macrophage marker MOMA-2. Positive staining was shown in brown and counter-stained with hemotoxilin

in blue. Enlarged details of the mgR/mgR sections are shown on the right. Scale bar: 50 μM.

Further, constant with cytokine and chemokine activation, macrophage recruitment was found in the media-adventitia border in mgR mutants (Figure 3.8). Together, these findings suggested presence of inflammatory events and activation of IL-6 signaling in TAAs in MFS.

3.2.3 IL-6 deficiency in mgR mutants decreases late-stage dilatation of ascending aorta without affecting survival.

In order to identify the role of IL-6 signaling in the formation and progression of aneurysmal dilatation, we bred mgR/mgR mice with IL-6-null mice to generate *Fbn1*$^{mgR/mgR}$:*Il6*$^{-/-}$ double mutant mouse line (DKOs). We first examined the activation of IL-6 signaling in the aortic tissues. With IHC staining of phospho-STAT3-Y705, an IL-6 downstream signaling molecule, we confirmed the inactivation of STAT3 phosphorylation induced by IL-6 (Figure 3.9).

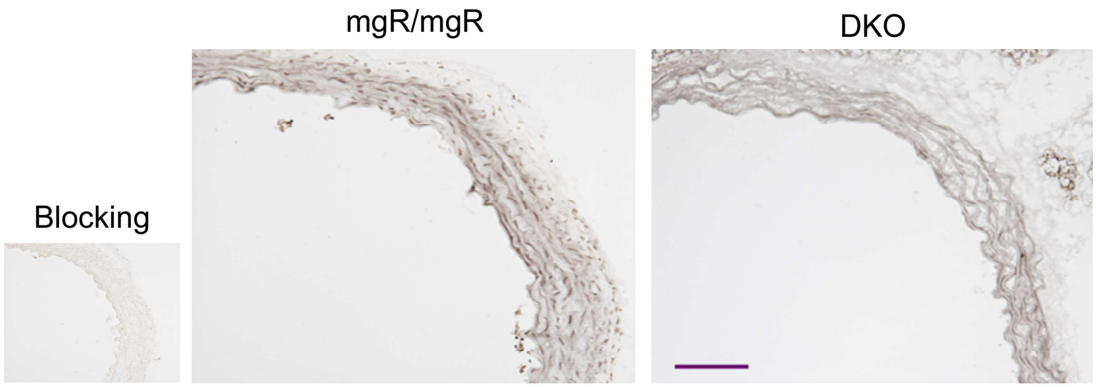

Figure 3.9. IHC staining of phospho-STAT3-Y705 in DKOs and mgR homozygotes. Positive staining was shown in grey. Aortic sections treated with p-STAT3 blocking peptide were shown on the left as negative control. n=4-6 in each group. Scale bar: 50 μM.

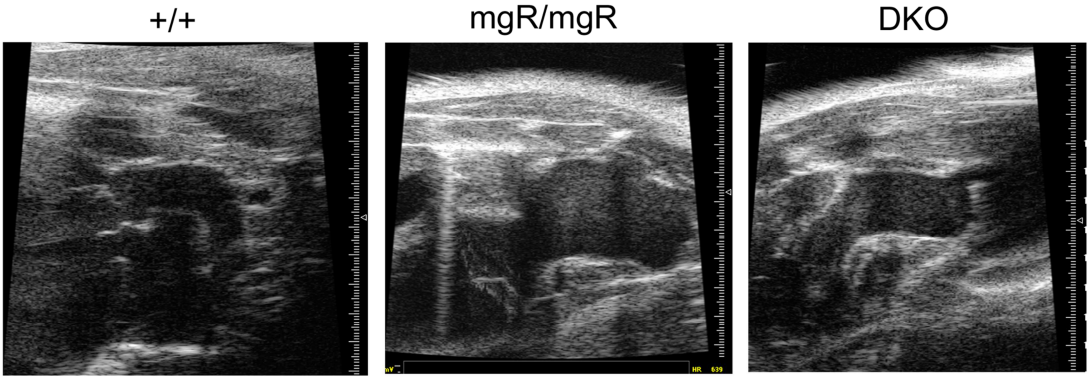

Figure 3.10. Representative images of echosonography of age-matched wild-type, mgR homozygotes and DKO mice.

We followed the progression of aortic dilation weekly using *in vivo* ultrasound imaging (Figure 3.10). As mgR mutants, these DKO mice developed spontaneous TAAs at 1-3 month of age. To our surprise, DKOs did not show improved survival, with median survival of 14 wk in DKOs and 11.5 wk in mgR/mgR mutants (Figure 3.11). DKOs also exhibited a similar rate of aneurysmal dilation at early stage of life (e.g. 5-12 wk, Figure 3.12). However, DKOs showed a significantly decreased size of ascending aorta at late stage of aneurysmal progression starting at 14 wk ($p<0.05$, Figure 3.12). These findings suggested that aortic dissection is not prevented, but delayed at a later time point, by IL-6 deficiency in DKOs.

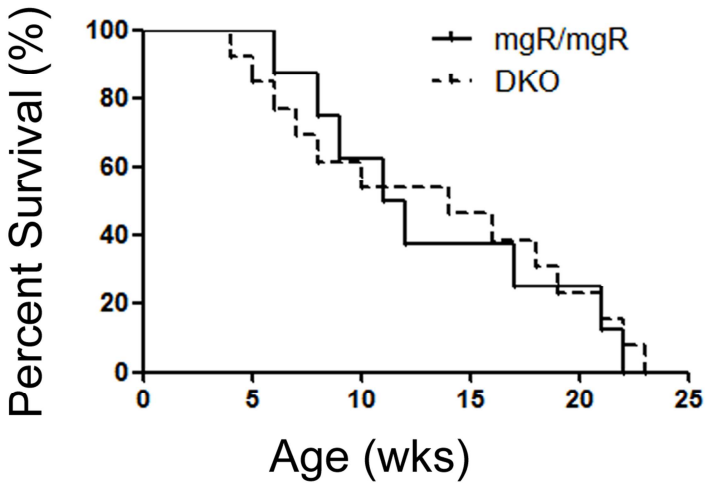

Figure 3.11. Survival curve of mgR homozygotes and DKOs. Survival of mgR homozygotes and DKOs were not significantly different. n=17-21 for each group.

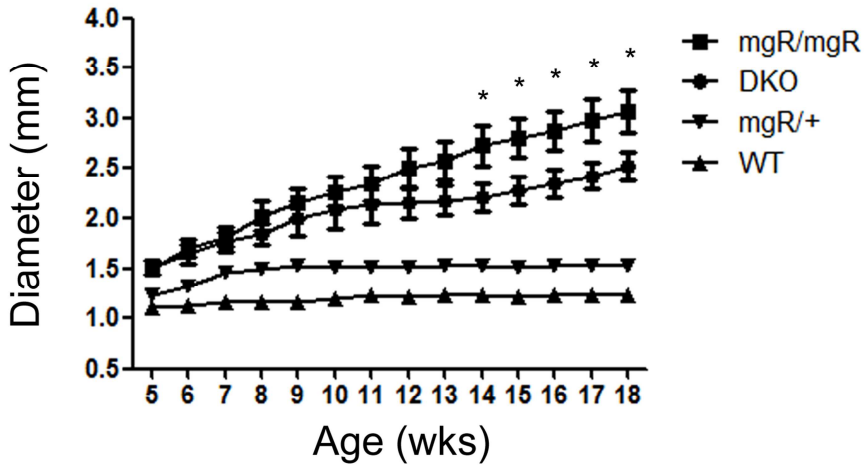

Figure 3.12. Dilatation of ascending aortas of DKOs and mgR mice. Diameters of ascending aorta were measured weekly *in vivo* by transthoracic echosonography. Progression of aortic dilation was recorded in mgR/mgR and DKO mice. n=10 for each group. *, $p<0.05$.

3.2.4 IL-6 deficiency leads to less ECM degeneration in mgR/mgR mice.

To investigate the molecular mechanisms of IL-6 deficiency-mediated delay of aneurysmal progression, we examined ECM components in the aortic wall. Using histological staining, we first observed a lower degree of elastin fiber breaks in the DKOs relative to mgR/mgR mice (Figure 3.13, $p<0.05$).

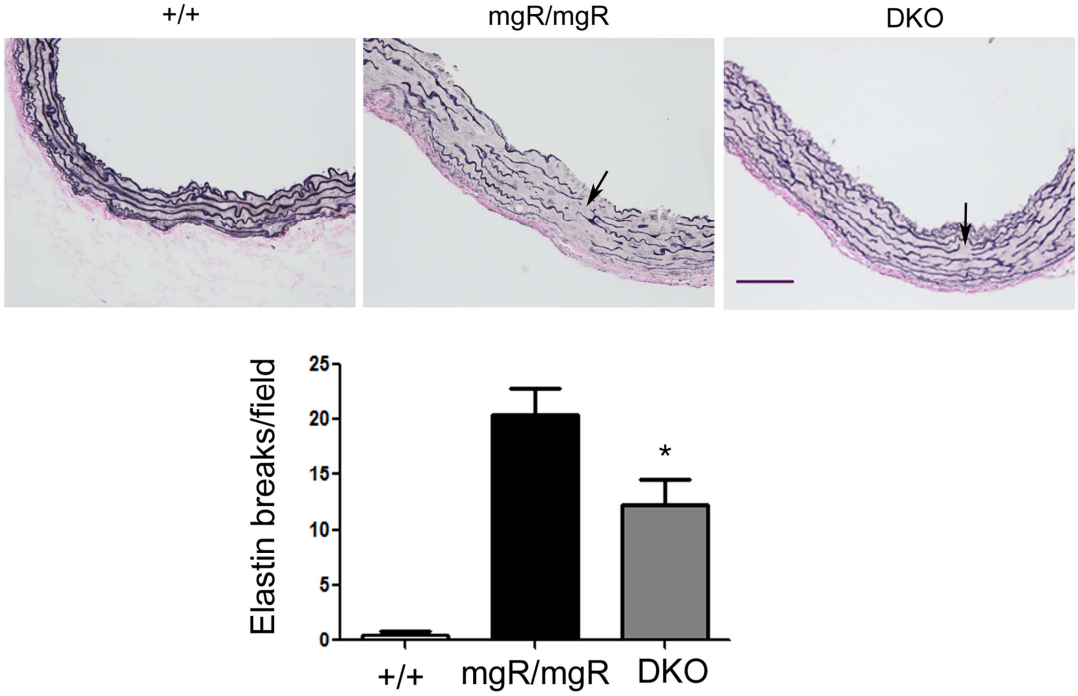

Figure 3.13. Elastin staining of ascending aortic sections of wild-type, mgR homozygotes and DKOs. Top panel: histological staining for elastin fibers in wild-type, mgR homozygotes and DKO mice. Bottom panel: breaking points in elastin fibers, as indicators of elastin degeneration, were quantified. n=6-7 in each group.

To more accurately evaluate structural elements of the aortic wall, we then performed three-dimensional imaging in ex vivo ascending aortas using MPA and SHG microscopy (Figure 3.14).

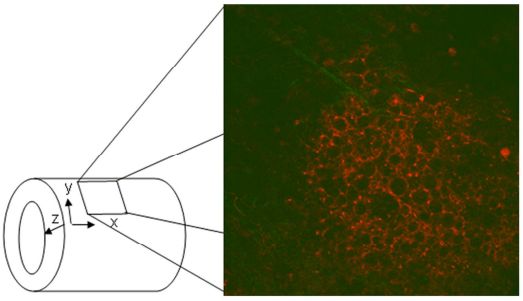
y
z
x

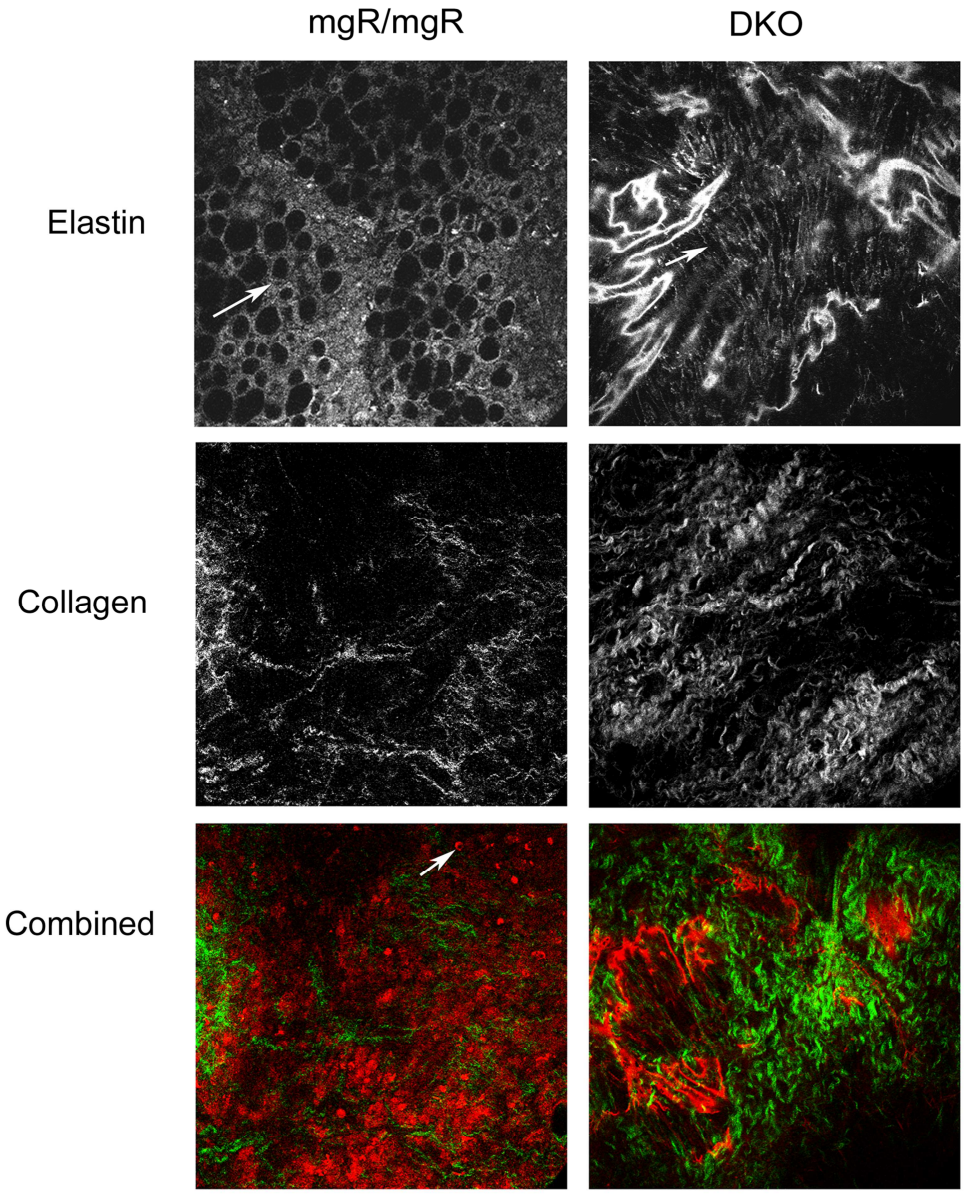
mgR/mgR
DKO
Elastin
Collagen
Combined

Figure 3.14. SHG and MPA microscopic images of mgR/mgR and age-matched DKO mice. Top panel: Elastin content was shown by MPA at the wavelength of 770 μM. Round and large hole formation is evident in mgR/mgR. In DKOs, Linear fissures were found in elastin sheets. Arrows: Degeneration tears and holes in elastin sheets. Middle panel: Collagen fibers. Bottom panel: Combined images of collagen and elastin at the adventitia-media border. Collagen was shown in green and elastin was shown in red. Arrows: Cell infiltration was more pronounced at the adventitia-media border in mgR/mgR mice. Shown is representative of 3 experiments for each group (n=4-6 in each group). Images were taken in 320X320 μM.

We found that in contrast to large hole-like structure of elastin degeneration in mgR/mgR mice, the DKOs developed only small gaps in the elastin sheets (Top panel, Figure 3.14).

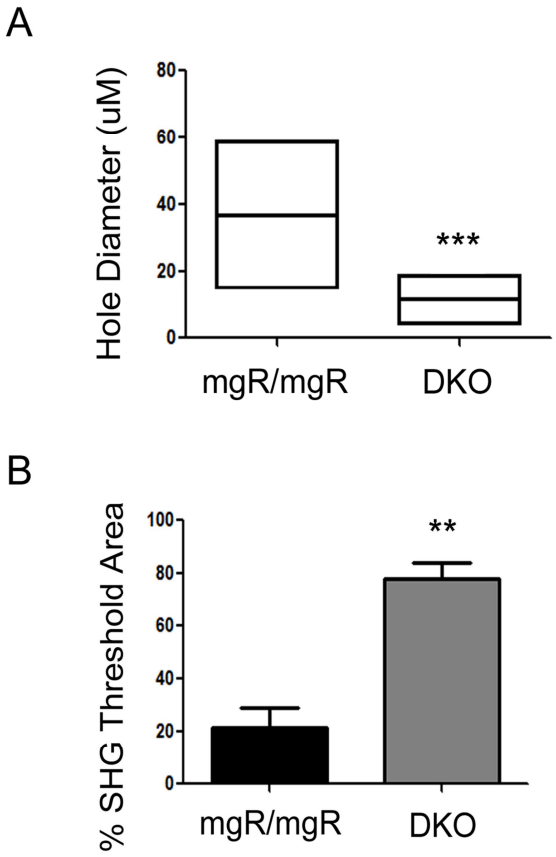

Figure 3.15. IL-6 deficiency led to less degree of elastin and collagen degradation. Sizes of holes and fissures in elastin sheets, indicators of elastin

degradation, were analyzed and quantified using MetaMorph Premier S software. Collagen contents in aortic samples were also measured as percentage of SHG signals. n=4-6 in each group. **, $p<0.01$. ***, $p<0.001$.

Moreover, the sizes of fissures were considerably smaller in the DKOs (Figure 3.15, $p<0.001$). In addition, there was a better preservation of collagen fibers in the adventitia as indicated by SHG signals (Figure 3.15, $p<0.01$). Finally, there was a lower number of autofluorescent infiltrating leukocytes in the border between media and adventitia, suggesting a less inflammatory phenotype (Bottom panel, Figure 3.1).

3.2.5 MMP-2 and MMP-9 activities are reduced in mgR/mgR mutants with IL-6 deficiency.

To test the mechanism for improved ECM preservation in DKOs, we evaluate activities of the MMP-2 and MMP-9 in aortic extracts. Gelatin zymography with ascending aortic samples from different genotypes showed significantly lower activities of both MMP-2 ($p<0.01$) and MMP-9 ($p<0.001$) in DKOs comparing with mgR/mgR mutants (Figure 3.16). Interestingly, there was also significant higher activities of MMP-2 and MMP-9 in mgR heterozygous mutants (mgR/+) relative to wild-type littermates (Figure 3.16, $p<0.05$, respectively), a phenomena consistent with significantly increased aortic dilation in mgR/+ comparing with wild-types (Figure 3.12, $p<0.001$).

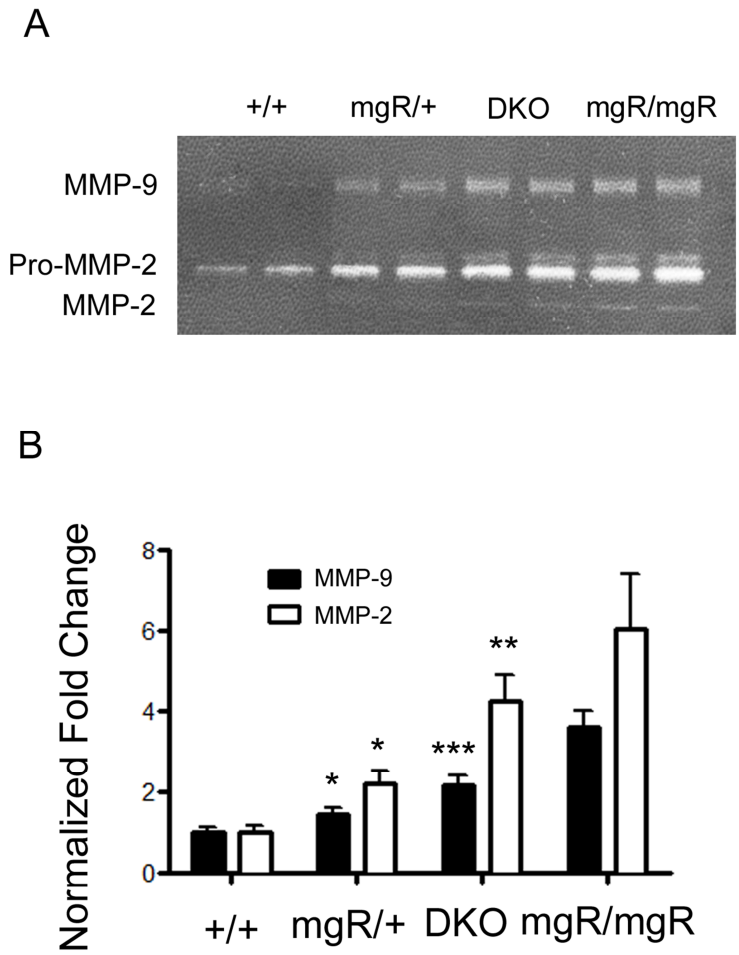

Figure 3.16. IL-6 deficiency led to lower MMP-2 and MMP-9 activities in DKOs comparing with mgR homozygotes. (A) Representative gelatin zymography of age-matched wild-type, mgR heterozygotes, mgR homozygotes and DKOs. Activities of Pro-MMP-2, MMP-2 and MMP-9 were shown. (B) Quantification of MMPs in different genotypes. n=5-8 in each group. *, $p<0.05$. **, $p<0.01$. ***, $p<0.001$.

3.3 DISCUSSION

Formation and dissection of thoracic aortic aneurysm are the most dangerous medical conditions caused by MFS. One of the major goals for developing treatments for

MFS is to delay aneurysmal dilation and prevent rupture. In this study, we reported the activation of IL-6-mediated inflammatory signaling in the ascending aortas in the mgR/mgR model of MFS. We have found that IL-6 deficiency in this model improved aortic pathology in decreasing ECM degeneration and leukocytic recruitment, reducing MMP-2 and MMP-9 expression and delaying late-stage aneurysmal dilation.

Recent studies have identified an inflammatory component in the etiology of TAA (Ejiri et al., 2003). In TAA patients undergoing surgical repair, enhanced expression of cytokines, such as IL-6 and interferon-γ (IFN-γ) are found in aortic tissues. These events are spatially correlated with increased monocyte/macrophage accumulation and enhanced MMP production. Homozygous mgR mice spontaneously die of dissecting TAAs, which exhibit leukocytic infiltration at advanced stage of disease progression (Pereira et al., 1999). Infiltrating leukocytes may accelerate pathogenesis by producing MMPs such as MMP-9 and stimulating degradation of elastic matrix. Matrix degenerated products, in turn, may be able to induce macrophage chemotaxis (Guo et al., 2006b; Guo et al., 2011), amplifying local inflammatory cascade.

Recently, enhanced Ang II signaling, a potent inducer of cytokines and chemokines, has been implicated in MFS. Aortic Ang II concentration is increased in mgR/mgR mice (Nagashima et al., 2001). Ang II type I receptor antagonist losartan and ACE inhibitor perindopril prevents aortic aneurysm formation in patients with MFS and reduce levels of TGF-β and MMPs (Habashi et al., 2006). In the aorta, Ang II activates NF-κB to regulate various inflammatory molecules including proinflammatory cytokines

(e.g. interleukins), chemokines (e.g. MCP-1, GM-CSF, etc.), adhesion molecules (e.g. E-selectin, ICAM-1, VCAM-1, etc.), and ECM-degrading MMPs. A major target of Ang II is to activate IL-6 expression by VSMCs, fibroblasts and recruited monocytes (Han et al., 1999). IL-6 is a 26 kDa glycosylated cytokine that activates Jak and STAT3, exerting diverse actions in multiple cell types. In the vessel, IL-6 promotes ROS production (Schrader et al., 2007) and macrophage differentiation, partially through induction of MCP-1 (Biswas et al., 1998; Tieu et al., 2009).

MMPs are capable of degrading the important structural components of the aortic wall, including elastin and collagen. MMP-2 is produced by medial VSMCs and adventitial fibroblasts (Rizas et al., 2009). MMP-2 is significantly elevated in TAA in MFS (Nataatmadja et al., 2006; Pereira et al., 1999), where it degrades elastin and collagen, destructing the medial and adventitial lamina. In addition, MMP-2 is capable of catalyzing the release of TGF-β from the latency-associated peptide (LAP) and activation of TGF-β. MMP-9 is also a strong elastin and collagen degrading enzyme that is mainly produced by infiltrating macrophages and neutrophils (Rizas et al., 2009). MMP-2 and MMP-9 levels are associated with sizes of TAA (Manning et al., 2003; Petersen et al., 2002). As direct targets of TGF-β, MMPs are elevated due to excessive TGF-β signaling in MFS (Kim et al., 2004). MMP-2 and MMP-9 activate TGF-β and degrade ECM, producing chemotactic fragment of matrix macromolecules (Guo et al., 2006b), further amplifying the inflammatory cascade.

In summary, our data suggested that in late stage of TAA, IL-6 mediated aortic inflammatory cytokine and chemokine expression, macrophage recruitment, ECM degeneration and levels of MMP-2 and MMP-9, thus contributing to aneurysmal dilation of the ascending aorta. IL-6 deficiency delayed, but did not prevent dissections or increase survival rate, suggesting the involvement of other important players in earlier stages of disease progression.

3.4 MATERIALS AND METHODS

3.4.1 Animal care and use

C57BL/6J wild type (WT; +/+) and *Il6*$^{-/-}$mice were obtained from The Jackson Laboratory. Heterozygotes mutant mice (*Fbn1*$^{mgR/+}$; mgR/+) were obtained from Johns Hopkins Univeristy and were bred to generate homozygous mutant mice (*Fbn1*$^{mgR/mgR}$; mgR/mgR) and wild-type littermates (*Fbn1*$^{+/+}$; +/+). To create *Il6*$^{-/-}$: *Fbn1*$^{mgR/mgR}$ double knockout (DKO) mice, Fbn1mgR/+ were bred with IL-6-null mice and offspring bred. For histological analysis of aortic tissues, mice were sacrificed at 12 weeks of age. This time point was chosen based on our preliminary studies in which aneurysmal changes were prominent and inflammatory events were evident. All animal experiments were approved by the University of Texas Medical Branch Institutional Animal Care and Use Committee. Mice were housed in the UTMB Animal Resource Center in accordance with the NIH Guidelines for the Care and Use of Animals in Research.

3.4.2 Echosonography

mgR/mgR, mgR/+, +/+ and DKO littermates were imaged weekly with noninvasive transthoracic ultrasound echosonographic techniques. Serial ultrasound imaging provided visualization of the progression of vessel dilatation. Mice were sedated with 1 % inhaled isoflurane delivered via nose cone and were positioned supine and imaged using Vevo 770 ultrasound machine for small animals (Visualsonics) equipped with a 707B transducer. Ascending aortas were imaged and diastolic diameter measured by two masked investigators in the both transverse and longitudinal axis view with B-mode and M-mode. Measurements were obtained in triplicate at the level of the ascending aorta.

3.4.3 Aortic explant and cytokine analysis

Following euthanasia and transcardial perfusion with PBS, the entire aorta was dissected and briefly cleaned under stereoscope. Thoracic aortas were isolated, immediately placed in 0.5 ml DMEM medium containing 1× ITS and 0.1 % BSA and incubated in a tissue culture hood at 37° C for 4 hrs as previously described (Tieu et al., 2009). Ex vivo explant culture medium was frozen at -80° C until being assayed for cytokines and chemokines using a multiplex, bead-based ELISA kit (Lincoplex/Millipore mouse cytokine panel) according to the manufacturers' instructions. Cytokine concentrations were determined relative to recombinant standards.

3.4.4 Immunohistochemistry (IHC) and elastin histological staining

Formalin-fixed, paraffin-embedded sections from ascending aortas were rehydrated using serial concentrations of ethanol. For histological staining, 5 μM

sections were staining with modified vrhoeff Van Gieson elastic stain kit (Sigma-Aldrich) using Van Gieson Solution, ferric chloride, alcoholic hematoxylin and Weigert's Iodine per manufacturers' instructions. Light microscopy was performed using 20X lens and quantification of elastin breaks was measured in triplicate by a masked investigator. For IHC, antigen retrieval was performed when necessary with antigen unmasking solution (Vector Laboratories). Paraffin-embedded sections were blocked using 0.1 % Triton-X, 5 % normal serum of the species producing the secondary antibodies and incubated with rabbit anti-IL-6 (1:600, Abcam) or rabbit anti-MCP-1 (1:100, Abcam). 7 μM-frozen sections of ascending aortas were blocked and stained with rat anti-macrophage (1:100, MOMA-2; Abcam) or rabbit phospho-STAT3-Tyr705 (D3A7, 1:100, Cell Signaling). In p-STAT3 staining, sections pre-treated with phospho-STAT3-Tyr705 blocking peptide (Cell Signaling) were used as negative controls. Biotinylated goat anti-rat or goat anti-rabbit antibodies (Vector Labs) were used as secondary antibodies, followed by staining with ABC and DAB kits (Vector Labs) per manufacturer's instructuctions. Secondary antibody-only controls were used to determine staining specificity.

3.4.5 Quantitative real-time PCR (Q-RT-PCR)

Ascending aortas were freshly isolated and frozen in -80° C for later use. Individual ascending aortas were pulverized in liquid nitrogen inside plastic pouches (Kapak SealPAK), further homogenized on ice in glass dounce homogenizers and RNA was extracted with TriReagent (Sigma-Aldrich) according to the manufacturer's instructions. RNA was quantified by Nanodrop (Thermo Scientific) and samples were

included when the 260/ 280 nm ratio was >1.6. Five μg RNA was reverse transcribed using Superscript III (Invitrogen) according to provided directions. Real-time PCR reactions were performed in triplicate using 1 μl of resulting cDNA per 20 μl reaction volume containing iQ SYBR Green Supermix (Bio-Rad). Primers were purchased from SABioscience for mouse ccl2/MCP-1 (PPM03151F) and mouse il6 (PPM03015A). Mouse Socs3 primers were synthesized (sense: 5'-CCGCGGGCACCTTTC-3'; anti-sense: 5'-TTGACGCTCAACGTGAAGAAGT-3'). PCR was performed on the CFX96 system (Bio-Rad) according to preset protocol. Data were normalized to the internal control GAPDH, and expressed as fold change calculated by the ΔΔCt method.

3.4.6 Multiphoton (MPA) microscopy and second harmonic generation (SHG)

The aortic arch of freshly isolated intact aorta was imaged using the nonlinear optical microscopy techniques of multiphoton microscopy and second harmonic generation microscopy with contrast based on intrinsic signals from the tissue (Zipfel et al., 2003). These include autofluorescence from elastin and the cytoplasm of cells in multiphoton autofluorescence microscopy (MPAM) and the frequency-doubled second harmonic generation signal that arises from fibrillar collagen (Campagnola and Loew, 2003). Used together, high-resolution images of the aortic media and adventitia can be obtained for assessment of depth-resolved structure (Boulesteix et al., 2006). MPAM/SHG evaluation was done with a customized Zeiss 410 confocal laser scanning inverted microscope modified for multiphoton excitation and detection along nondescanned optics (Sun et al., 2004). Briefly, illumination was from a femtosecond titanium sapphire laser (Tsunami, SpectralPhysics) having a 5W frequency-doubled

Nd:YVO pump laser, and routed into the scanhead and through the sample objective using optics for ultrafast laser propagation. The system operated with a typical pulse width of 140 fs prior to the objective (40x 1.2 N.A. water). Excitation for autofluorescence was 780 nm and for SHG was 840 nm. An epi-configuration was used for collection of emitted light and detected using a cooled PMT placed in a nondescanned configuration (R6060, Hamamatsu, Japan). Fluorescence emission in the spectral region of 450-650 nm was collected for detection of broadband autofluorecence from the aorta. Second harmonic generation was collected using a 420+/-14nm bandpass filter in the nondescanned detector path. Thus, MPAM and SHG image stacks were taken sequentially. The intact aorta was placed on a 35 mm imaging dish having a #1.5 coverslip bottom (Matek, Ashland, MA) and immersed in phosphate buffered saline. Image stack were obtained beginning prior to the adventitial surface and into the aorta using a step size of 1 µm to depths > 150 µm. The objective provided a field of view of 320x320 µm. Image reconstructions of micrograph stacks were constructed using Metamorph (Molecular Devices, Sunnyvale CA). Analysis of features found in the elastin lamellae was performed on Metamorph using the measurement tools to calculate diameter of holes and represented in µm. SHG signal content was quantified by first thresholding SHG images to determine the regions positive for fibrillar collagen. The same thresholding parameters were used for the full stack and between samples. The percent area positive for collagen according to the threshold region was determined relative to the full field. A value per group was obtained by averaging this area between samples of a group.

3.4.7 Gelatin Zymography

Aortic proteins from 12-week +/+, mgR/+, mgR/mgR and DKO littermates were exacted as previously described (Davis et al., 1998). Protein concentrations were standardized with Bio-Rad protein assay. Equal amounts (25 μg) of aortic proteins were electrophoresized on 10% gelatin zymogram gels (Invitrogen) as previously described (Hu and Beeton, 2010). The molecular sizes were determined using protein standards (Invitrogen). Gels were scanned and shown in black and white for densitometry analysis by ImageJ.

3.4.8 Data analysis

Data are reported as ± SEM. Differences between 2 groups were analyzed by Student's t test (2-tail, assuming unequal variances). One-way ANOVA was performed when comparing multiple groups, followed by Tukey or Bonferroni post-hoc tests to determine significance. Kaplan-Meier survival curves for different genotypes were plotted and significance analyzed with Mantel-Cox test. In all cases, $p < 0.05$ was considered significant.

Chapter 4

Summary and Future Directions

4.1 SUMMARY

As a member of a cardioactive cytokine superfamily including cardiotropin, IL-11, and -12, and G-CSF, IL-6 binds to unique alpha receptors and mediates it actions through a common gp130 signal transducer (Mihara et al., 2012). By activating its classical signaling pathways, IL-6 targets various types of vascular cells include vascular smooth muscle cells, endothelial cells, and infiltrating monocyte/macrophage populations. In cardiovascular diseases, IL-6 is identified as an independent biomarker of vascular atherosclerotic risk and for aneurysmal diseases (Norgren and Swartbol, 1997; Schuett et al., 2009). Recently, we demonstrated that IL-6 was a highly upregulated cytokine in Ang II-stimulated vessels (Recinos et al., 2007; Tieu et al., 2009) and that IL-6 plays a major pathogenic role in aortic aneurysms induced by Ang II because its deficiency significantly blocked monocyte infiltration, reactive oxygen species (ROS) formation, chemotactic cytokine amplification and aortic dissections (Tieu et al., 2009). In this study, we explored the precise mechanisms by which IL-6 signaling induces leukocyte recruitment and facilitates aneurysmal formation and progression.

In a normolipidemic mouse model of Ang II-induced aortic aneurysms and dissections, we tested the relationship of IL-6 signaling on formation of the Th17 cell population, and the pathogenic role of IL-6-mediated IL-17A signaling in aortic aneurysms and dissections. We reported that Ang II infusion induced local IL-6 production, aortic dissections and CD4+-interleukin 17A (IL-17A)-expressing, Th17 cell accumulation in C57BL/6 mice. A blunted local Th17 activation, macrophage recruitment, and reduced incidence of aortic dissections were seen in *Il6*$^{-/-}$ mice in the

C57BL/6 background. To determine pathological roles of Th17 lymphocytes, we reported that mice treated with IL-17A neutralizing antibodies, or those genetically deficient in IL-17A showed decreased aortic chemokine MCP-1 production and macrophage recruitment, leading to a reduction in aortic dissections. We also showed increased Th17 infiltration into the aortic adventitial-medial border in patients with ascending aortic dissections. These results indicate that, in Ang II-induced aortic aneurysms and dissections, IL-6 signaling converges on Th17 recruitment and IL-17A signaling upstream of macrophage recruitment, mediating vascular inflammation and aortic dissections.

In another mouse model with thoracic aortic aneurysm caused by *Fbn-1* gene mutation (the mgR homozygotes), we explored the role of IL-6 in aortic structural remodeling and development of ascending aortic dissections. Using Q-RT-PCR, ELISA and IHC techniques, we found that the expression and secretion of IL-6 and MCP-1 are elevated in thoracic aneurysmal tissues. Additionally, we observed significant macrophage recruitment in aneurysmal aortic wall in advanced stage of disease progression. To study the role of IL-6 signaling, we generated mgR homozygotes with IL-6 deficiency (DKOs). We found that DKOs showed a decrease in aortic dilation at late stage of disease without affecting survival rate. We also reported that DKOs exhibited a lower degree of elastin and collagen degeneration comparing with mgR homozygotes. Finally, we showed that the better preservation of ECM proteins was associated with decreased activities of MMP-2 and MMP-9. These findings suggest that activation of IL-6-mediated inflammatory signaling contributed to aneurysmal

progression in MFS through recruitment of leukocytes and stimulating MMP expression, thus aggravating ECM degradation.

In summary, our findings on these two research projects demonstrate that IL-6 is an important pro-inflammatory cytokine that is involved in immune cell recruitment, matrix remodeling and aneurysm development. By inducing Th17 activation and differentiation in local aneurysmal tissue, IL-6 mediates vascular IL-17 production, which may further facilitate monocyte recruitment and macrophage activation. On the other hand, IL-6 regulates MMP activation in aneurysms caused by MFS, leading to enhanced matrix degeneration and contributing to aneurysmal progression.

4.2 Future Directions

4.2.1 Role of IL-6-STAT3 signaling pathways in Ang II-induced vascular inflammation

IL-6 signals through classical signaling pathway or the alternative signaling pathways which involves binding to the membrane-bound IL-6 receptor or the soluble IL-6 receptor, subsequent phosphorylation of Jak kinase and activation of STAT3. Our preliminary studies have shown that STAT3 phosphorylation at tyrosine residue 705 is enhanced in Ang II-treated aortic tissues. Future studies using STAT3 phosphorylation inhibitors should be conducted to examine the roles of IL-6-STAT3 signaling activation in aortic macrophage recruitment, T cell activation and vascular inflammation.

4.2.2 Role of NF-κB activation in Ang II-induced vascular inflammation

Our group has established that Ang II signals through the activation of the NF-κB transcription factor in VSMCs. A major event during this process is phosphorylation of RelA subunit at serine residue 536. Our preliminary studies showed that in Ang II-treated aortic tissues, RelA phosphorylation is observed in both VSMCs and adventitial fibroblasts. Due to the important role of adventitial fibroblasts in production of IL-6, MCP-1, and cross-talk with macrophages, we proposed that activation of NF-κB signaling activation in fibroblast cells is critical to mediate vascular inflammatory events such as leukocyte chemotaxis, differentiation and local activation. In order to test the role of NF-κB signaling in fibroblasts, we designed and created a fibroblast cell-specific, Cre-inducible conditional knock-out mouse line in which the expression of *Rela* can be abolished in fibroblasts. Further experimentation should be performed using this line to test the role of NF-κB signaling in fibroblasts in Ang II-induced vascular inflammation.

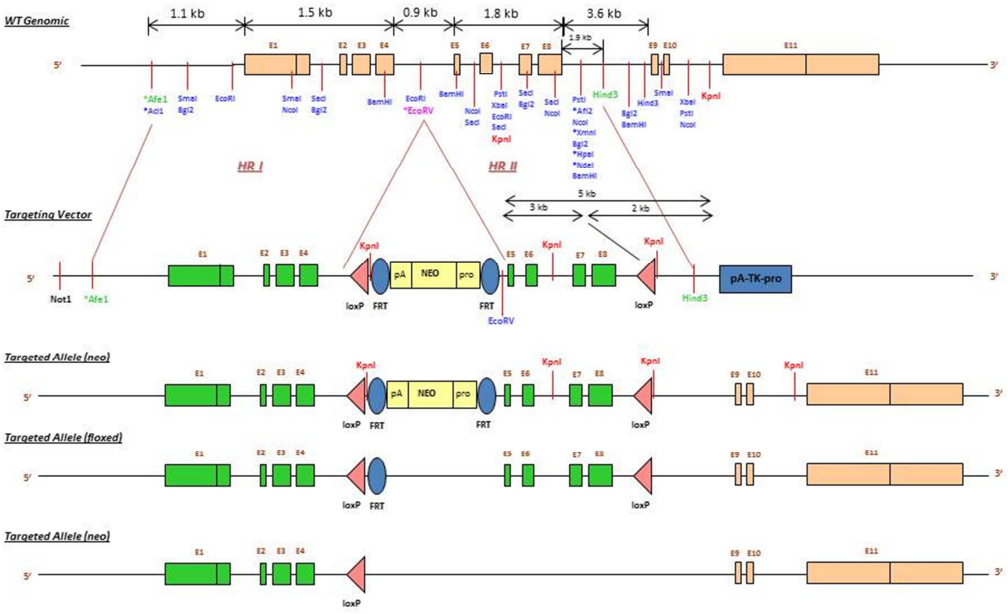

Figure 4.1. Schematic diagram of construction and generation of conditional RelA-targeted mouse line.

4.2.3 Cellular mechanisms of vascular Th17 activation

Our preliminary studies have shown that during the processes of Ang II-induced aortic remodeling, adventitial fibroblasts obtained contractile activities and transdifferentiate into myofibroblasts. Myofibroblasts, when in close proximity to T cells, are reported to be capable of inducing naïve T cell differentiation into Th17 cells. To explore the cellular mechanisms of vascular Th17 activation, we proposed that the interaction between aortic myofibroblasts and naïve T cells potentiates local IL-17 expression and facilitates Th17 polarization. Further co-culture experiments of adventitial myofibroblasts and T cells should be performed to investigate the role of cell-cell interaction during the vascular inflammatory processes.

References

Biswas, P., F. Delfanti, S. Bernasconi, M. Mengozzi, M. Cota, N. Polentarutti, A. Mantovani, A. Lazzarin, S. Sozzani, and G. Poli. 1998. Interleukin-6 induces monocyte chemotactic protein-1 in peripheral blood mononuclear cells and in the U937 cell line. *Blood*. 91:258-265.

Booms, P., A. Ney, F. Barthel, G. Moroy, D. Counsell, C. Gille, G. Guo, R. Pregla, S. Mundlos, A.J. Alix, and P.N. Robinson. 2006. A fibrillin-1-fragment containing the elastin-binding-protein GxxPG consensus sequence upregulates matrix metalloproteinase-1: biochemical and computational analysis. *Journal of molecular and cellular cardiology*. 40:234-246.

Booms, P., R. Pregla, A. Ney, F. Barthel, D.P. Reinhardt, A. Pletschacher, S. Mundlos, and P.N. Robinson. 2005. RGD-containing fibrillin-1 fragments upregulate matrix metalloproteinase expression in cell culture: a potential factor in the pathogenesis of the Marfan syndrome. *Human genetics*. 116:51-61.

Boring, L., J. Gosling, M. Cleary, and I.F. Charo. 1998. Decreased lesion formation in CCR2-/- mice reveals a role for chemokines in the initiation of atherosclerosis. *Nature*. 394:894-897.

Boulanger, M.J., D.C. Chow, E.E. Brevnova, and K.C. Garcia. 2003. Hexameric structure and assembly of the interleukin-6/IL-6 alpha-receptor/gp130 complex. *Science*. 300:2101-2104.

Boulesteix, T., A.M. Pena, N. Pages, G. Godeau, M.P. Sauviat, E. Beaurepaire, and M.C. Schanne-Klein. 2006. Micrometer scale ex vivo multiphoton imaging of unstained arterial wall structure. *Cytometry. Part A : the journal of the International Society for Analytical Cytology*. 69:20-26.

Brasier, A.R. 2010. The nuclear factor-kappaB-interleukin-6 signalling pathway mediating vascular inflammation. *Cardiovascular research*. 86:211-218.

Brasier, A.R., A. Recinos, 3rd, and M.S. Eledrisi. 2002. Vascular inflammation and the renin-angiotensin system. *Arteriosclerosis, thrombosis, and vascular biology*. 22:1257-1266.

Brown, R.M., Jr., A.C. Millard, and P.J. Campagnola. 2003. Macromolecular structure of cellulose studied by second-harmonic generation imaging microscopy. *Optics letters*. 28:2207-2209.

Butcher, M.J., B.N. Gjurich, T. Phillips, and E.V. Galkina. 2012. The IL-17A/IL-17RA Axis Plays a Proatherogenic Role via the Regulation of Aortic Myeloid Cell Recruitment. *Circulation research.*

Campagnola, P.J., and L.M. Loew. 2003. Second-harmonic imaging microscopy for visualizing biomolecular arrays in cells, tissues and organisms. *Nature biotechnology*. 21:1356-1360.

Carvajal, G., J. Rodriguez-Vita, R. Rodrigues-Diez, E. Sanchez-Lopez, M. Ruperez, C. Cartier, V. Esteban, A. Ortiz, J. Egido, S.A. Mezzano, and M. Ruiz-Ortega. 2008. Angiotensin II activates the Smad pathway during epithelial mesenchymal transdifferentiation. *Kidney international*. 74:585-595.

Cassis, L.A., M. Gupte, S. Thayer, X. Zhang, R. Charnigo, D.A. Howatt, D.L. Rateri, and A. Daugherty. 2009. ANG II infusion promotes abdominal aortic aneurysms independent of increased blood pressure in hypercholesterolemic mice. *American journal of physiology. Heart and circulatory physiology*. 296:H1660-1665.

Chan, Y.K., P.F. Davis, S.D. Poppitt, X. Sun, N.S. Greenhill, R. Krishnamurthi, A. Przepiorski, A.T. McGill, and G.W. Krissansen. 2012. Influence of tail versus cardiac sampling on blood glucose and lipid profiles in mice. *Laboratory animals*.

Chen, H.J., D.Y. Li, T. Saldeen, M.I. Phillips, and J.L. Mehta. 2001. Attenuation of tissue P-selectin and MCP-1 expression and intimal proliferation by AT(1) receptor blockade in hyperlipidemic rabbits. *Biochemical and biophysical research communications*. 282:474-479.

Chen, S., T.R. Crother, and M. Arditi. 2010a. Emerging role of IL-17 in atherosclerosis. *Journal of innate immunity*. 2:325-333.

Chen, S., K. Shimada, W. Zhang, G. Huang, T.R. Crother, and M. Arditi. 2010b. IL-17A is proatherogenic in high-fat diet-induced and Chlamydia pneumoniae infection-accelerated atherosclerosis in mice. *J Immunol*. 185:5619-5627.

Cheng, X., X. Yu, Y.J. Ding, Q.Q. Fu, J.J. Xie, T.T. Tang, R. Yao, Y. Chen, and Y.H. Liao. 2008. The Th17/Treg imbalance in patients with acute coronary syndrome. *Clinical Immunology*. 127:89-97.

Chomarat, P., J. Banchereau, J. Davoust, and A.K. Palucka. 2000. IL-6 switches the differentiation of monocytes from dendritic cells to macrophages. *Nat Immunol*. 1:510-514.

Chung, A.W., H.H. Yang, M.W. Radomski, and C. van Breemen. 2008. Long-term doxycycline is more effective than atenolol to prevent thoracic aortic aneurysm in marfan syndrome through the inhibition of matrix metalloproteinase-2 and -9. *Circulation research*. 102:e73-85.

Daugherty, A., and L.A. Cassis. 2002. Mechanisms of abdominal aortic aneurysm formation. *Current atherosclerosis reports*. 4:222-227.

Daugherty, A., M.W. Manning, and L.A. Cassis. 2000. Angiotensin II promotes atherosclerotic lesions and aneurysms in apolipoprotein E-deficient mice. *J Clin Invest*. 105:1605-1612.

Daugherty, A., D.L. Rateri, I.F. Charo, A.P. Owens, D.A. Howatt, and L.A. Cassis. 2010. Angiotensin II infusion promotes ascending aortic aneurysms: attenuation by CCR2 deficiency in apoE-/- mice. *Clin Sci (Lond)*. 118:681-689.

Daugherty, A., B.S. Zweifel, and G. Schonfeld. 1991. The effects of probucol on the progression of atherosclerosis in mature Watanabe heritable hyperlipidaemic rabbits. *British journal of pharmacology*. 103:1013-1018.

Davis, V., R. Persidskaia, L. Baca-Regen, Y. Itoh, H. Nagase, Y. Persidsky, A. Ghorpade, and B.T. Baxter. 1998. Matrix metalloproteinase-2 production and its binding to the matrix are increased in abdominal aortic aneurysms. *Arteriosclerosis, thrombosis, and vascular biology*. 18:1625-1633.

Dawson, J., G. Cockerill, E. Choke, I. Loftus, and M.M. Thompson. 2006. Aortic aneurysms as a source of circulating interleukin-6. *Annals of the New York Academy of Sciences*. 1085:320-323.

Dawson, J., G.W. Cockerill, E. Choke, A.M. Belli, I. Loftus, and M.M. Thompson. 2007. Aortic aneurysms secrete interleukin-6 into the circulation. *Journal of vascular surgery : official publication, the Society for Vascular Surgery [and] International Society for Cardiovascular Surgery, North American Chapter*. 45:350-356.

Dietz, H.C., B. Loeys, L. Carta, and F. Ramirez. 2005. Recent progress towards a molecular understanding of Marfan syndrome. *American journal of medical genetics. Part C, Seminars in medical genetics*. 139C:4-9.

Dietz, H.C., and R.E. Pyeritz. 1995. Mutations in the human gene for fibrillin-1 (FBN1) in the Marfan syndrome and related disorders. *Human molecular genetics*. 4 Spec No:1799-1809.

Eid, R.E., D.A. Rao, J. Zhou, S.F. Lo, H. Ranjbaran, A. Gallo, S.I. Sokol, S. Pfau, J.S. Pober, and G. Tellides. 2009. Interleukin-17 and interferon-gamma are produced concomitantly by human coronary artery-infiltrating T cells and act synergistically on vascular smooth muscle cells. *Circulation*. 119:1424-1432.

Ejiri, J., N. Inoue, T. Tsukube, T. Munezane, Y. Hino, S. Kobayashi, K. Hirata, S. Kawashima, S. Imajoh-Ohmi, Y. Hayashi, H. Yokozaki, Y. Okita, and M. Yokoyama. 2003. Oxidative stress in the pathogenesis of thoracic aortic aneurysm: protective role of statin and angiotensin II type 1 receptor blocker. *Cardiovascular research*. 59:988-996.

Erbel, C., L. Chen, F. Bea, S. Wangler, S. Celik, F. Lasitschka, Y. Wang, D. Bockler, H.A. Katus, and T.J. Dengler. 2009. Inhibition of IL-17A attenuates

atherosclerotic lesion development in apoE-deficient mice. *J Immunol*. 183:8167-8175.

Gaffen, S.L. 2009. Structure and signalling in the IL-17 receptor family. *Nature reviews. Immunology*. 9:556-567.

Galle, C., L. Schandene, P. Stordeur, Y. Peignois, J. Ferreira, J.C. Wautrecht, J.P. Dereume, and M. Goldman. 2005. Predominance of type 1 CD4+ T cells in human abdominal aortic aneurysm. *Clin Exp Immunol*. 142:519-527.

Ge, G., and D.S. Greenspan. 2006. BMP1 controls TGFbeta1 activation via cleavage of latent TGFbeta-binding protein. *The Journal of cell biology*. 175:111-120.

Guo, D.C., C.L. Papke, R. He, and D.M. Milewicz. 2006a. Pathogenesis of thoracic and abdominal aortic aneurysms. *Annals of the New York Academy of Sciences*. 1085:339-352.

Guo, G., P. Booms, M. Halushka, H.C. Dietz, A. Ney, S. Stricker, J. Hecht, S. Mundlos, and P.N. Robinson. 2006b. Induction of macrophage chemotaxis by aortic extracts of the mgR Marfan mouse model and a GxxPG-containing fibrillin-1 fragment. *Circulation*. 114:1855-1862.

Guo, G., P. Gehle, S. Doelken, J.L. Martin-Ventura, Y. von Kodolitsch, R. Hetzer, and P.N. Robinson. 2011. Induction of macrophage chemotaxis by aortic extracts from patients with Marfan syndrome is related to elastin binding protein. *PloS one*. 6:e20138.

Guzik, T.J., N.E. Hoch, K.A. Brown, L.A. McCann, A. Rahman, S. Dikalov, J. Goronzy, C. Weyand, and D.G. Harrison. 2007. Role of the T cell in the genesis of

angiotensin II induced hypertension and vascular dysfunction. *The Journal of experimental medicine*. 204:2449-2460.

Habashi, J.P., D.P. Judge, T.M. Holm, R.D. Cohn, B.L. Loeys, T.K. Cooper, L. Myers, E.C. Klein, G. Liu, C. Calvi, M. Podowski, E.R. Neptune, M.K. Halushka, D. Bedja, K. Gabrielson, D.B. Rifkin, L. Carta, F. Ramirez, D.L. Huso, and H.C. Dietz. 2006. Losartan, an AT1 antagonist, prevents aortic aneurysm in a mouse model of Marfan syndrome. *Science*. 312:117-121.

Hall, J.E., H.L. Mizelle, M.W. Brands, and D.A. Hildebrandt. 1992. Pressure natriuresis and angiotensin II in reduced kidney mass, salt-induced hypertension. *The American journal of physiology*. 262:R61-71.

Han, Y., M.S. Runge, and A.R. Brasier. 1999. Angiotensin II induces interleukin-6 transcription in vascular smooth muscle cells through pleiotropic activation of nuclear factor-kappa B transcription factors. *Circulation research*. 84:695-703.

He, R., D.C. Guo, A.L. Estrera, H.J. Safi, T.T. Huynh, Z. Yin, S.N. Cao, J. Lin, T. Kurian, L.M. Buja, Y.J. Geng, and D.M. Milewicz. 2006. Characterization of the inflammatory and apoptotic cells in the aortas of patients with ascending thoracic aortic aneurysms and dissections. *The Journal of thoracic and cardiovascular surgery*. 131:671-678.

He, R., D.C. Guo, W. Sun, C.L. Papke, S. Duraisamy, A.L. Estrera, H.J. Safi, C. Ahn, L.M. Buja, F.C. Arnett, J. Zhang, Y.J. Geng, and D.M. Milewicz. 2008. Characterization of the inflammatory cells in ascending thoracic aortic aneurysms in patients with Marfan syndrome, familial thoracic aortic aneurysms, and

sporadic aneurysms. *The Journal of thoracic and cardiovascular surgery*. 136:922-929, 929 e921.

Hirata, K., F. Triposkiadis, E. Sparks, J. Bowen, C.F. Wooley, and H. Boudoulas. 1991. The Marfan syndrome: abnormal aortic elastic properties. *Journal of the American College of Cardiology*. 18:57-63.

Hofstetter, H.H., S.M. Ibrahim, D. Koczan, N. Kruse, A. Weishaupt, K.V. Toyka, and R. Gold. 2005. Therapeutic efficacy of IL-17 neutralization in murine experimental autoimmune encephalomyelitis. *Cellular immunology*. 237:123-130.

Hou, T., B.C. Tieu, S. Ray, A. Recinos Iii, R. Cui, R.G. Tilton, and A.R. Brasier. 2008. Roles of IL-6-gp130 Signaling in Vascular Inflammation. *Curr Cardiol Rev*. 4:179-192.

Hu, X., and C. Beeton. 2010. Detection of functional matrix metalloproteinases by zymography. *Journal of visualized experiments : JoVE*.

Ikonomidis, J.S., J.A. Jones, J.R. Barbour, R.E. Stroud, L.L. Clark, B.S. Kaplan, A. Zeeshan, J.E. Bavaria, J.H. Gorman, 3rd, F.G. Spinale, and R.C. Gorman. 2006. Expression of matrix metalloproteinases and endogenous inhibitors within ascending aortic aneurysms of patients with Marfan syndrome. *Circulation*. 114:I365-370.

Ishibashi, M., K. Egashira, Q. Zhao, K. Hiasa, K. Ohtani, Y. Ihara, I.F. Charo, S. Kura, T. Tsuzuki, A. Takeshita, and K. Sunagawa. 2004. Bone marrow-derived monocyte chemoattractant protein-1 receptor CCR2 is critical in angiotensin II-induced

acceleration of atherosclerosis and aneurysm formation in hypercholesterolemic mice. *Arteriosclerosis, thrombosis, and vascular biology*. 24:e174-178.

Jones, K.G., D.J. Brull, L.C. Brown, M. Sian, R.M. Greenhalgh, S.E. Humphries, and J.T. Powell. 2001. Interleukin-6 (IL-6) and the prognosis of abdominal aortic aneurysms. *Circulation*. 103:2260-2265.

Kaartinen, V., and D. Warburton. 2003. Fibrillin controls TGF-beta activation. *Nature genetics*. 33:331-332.

Kim, H.S., T. Shang, Z. Chen, S.C. Pflugfelder, and D.Q. Li. 2004. TGF-beta1 stimulates production of gelatinase (MMP-9), collagenases (MMP-1, -13) and stromelysins (MMP-3, -10, -11) by human corneal epithelial cells. *Experimental eye research*. 79:263-274.

Kossakowska, A.E., D.R. Edwards, C. Prusinkiewicz, M.C. Zhang, D. Guo, S.J. Urbanski, T. Grogan, L.A. Marquez, and A. Janowska-Wieczorek. 1999. Interleukin-6 regulation of matrix metalloproteinase (MMP-2 and MMP-9) and tissue inhibitor of metalloproteinase (TIMP-1) expression in malignant non-Hodgkin's lymphomas. *Blood*. 94:2080-2089.

Kouchoukos, N.T., J.E. Bavaria, J.S. Coselli, R. De La Torre, J.S. Ikonomidis, R.C. Karmy-Jones, R.S. Mitchell, R.J. Shemin, D. Spielvogel, L.G. Svensson, and G.H. Wheatley. 2006. Guidelines for credentialing of practitioners to perform endovascular stent-grafting of the thoracic aorta. *The Annals of thoracic surgery*. 81:1174-1176.

Kuivaniemi, H., C.D. Platsoucas, and M.D. Tilson, 3rd. 2008. Aortic aneurysms: an immune disease with a strong genetic component. *Circulation*. 117:242-252.

Kusano, K., C. Miyaura, M. Inada, T. Tamura, A. Ito, H. Nagase, K. Kamoi, and T. Suda. 1998. Regulation of matrix metalloproteinases (MMP-2, -3, -9, and -13) by interleukin-1 and interleukin-6 in mouse calvaria: association of MMP induction with bone resorption. *Endocrinology*. 139:1338-1345.

Longo, G.M., W. Xiong, T.C. Greiner, Y. Zhao, N. Fiotti, and B.T. Baxter. 2002. Matrix metalloproteinases 2 and 9 work in concert to produce aortic aneurysms. *The Journal of clinical investigation*. 110:625-632.

Madhur, M.S., S.A. Funt, L. Li, A. Vinh, W. Chen, H.E. Lob, Y. Iwakura, Y. Blinder, A. Rahman, A.A. Quyyumi, and D.G. Harrison. 2011. Role of interleukin 17 in inflammation, atherosclerosis, and vascular function in apolipoprotein e-deficient mice. *Arteriosclerosis, thrombosis, and vascular biology*. 31:1565-1572.

Madhur, M.S., H.E. Lob, L.A. McCann, Y. Iwakura, Y. Blinder, T.J. Guzik, and D.G. Harrison. 2010. Interleukin 17 promotes angiotensin II-induced hypertension and vascular dysfunction. *Hypertension*. 55:500-507.

Maiellaro, K., and W.R. Taylor. 2007. The role of the adventitia in vascular inflammation. *Cardiovascular research*. 75:640-648.

Manning, M.W., L.A. Cassis, and A. Daugherty. 2003. Differential effects of doxycycline, a broad-spectrum matrix metalloproteinase inhibitor, on angiotensin II-induced atherosclerosis and abdominal aortic aneurysms. *Arterioscler Thromb Vasc Biol*. 23:483-488.

Mihara, M., M. Hashizume, H. Yoshida, M. Suzuki, and M. Shiina. 2012. IL-6/IL-6 receptor system and its role in physiological and pathological conditions. *Clin Sci (Lond)*. 122:143-159.

Mizuguchi, T., G. Collod-Beroud, T. Akiyama, M. Abifadel, N. Harada, T. Morisaki, D. Allard, M. Varret, M. Claustres, H. Morisaki, M. Ihara, A. Kinoshita, K. Yoshiura, C. Junien, T. Kajii, G. Jondeau, T. Ohta, T. Kishino, Y. Furukawa, Y. Nakamura, N. Niikawa, C. Boileau, and N. Matsumoto. 2004. Heterozygous TGFBR2 mutations in Marfan syndrome. *Nature genetics*. 36:855-860.

Nagashima, H., Y. Sakomura, Y. Aoka, K. Uto, K. Kameyama, M. Ogawa, S. Aomi, H. Koyanagi, N. Ishizuka, M. Naruse, M. Kawana, and H. Kasanuki. 2001. Angiotensin II type 2 receptor mediates vascular smooth muscle cell apoptosis in cystic medial degeneration associated with Marfan's syndrome. *Circulation*. 104:I282-287.

Nakae, S., Y. Komiyama, A. Nambu, K. Sudo, M. Iwase, I. Homma, K. Sekikawa, M. Asano, and Y. Iwakura. 2002. Antigen-specific T cell sensitization is impaired in IL-17-deficient mice, causing suppression of allergic cellular and humoral responses. *Immunity*. 17:375-387.

Nataatmadja, M., J. West, and M. West. 2006. Overexpression of transforming growth factor-beta is associated with increased hyaluronan content and impairment of repair in Marfan syndrome aortic aneurysm. *Circulation*. 114:I371-377.

Norgren, L., and P. Swartbol. 1997. Biological responses to endovascular treatment of abdominal aortic aneurysms. *Journal of endovascular surgery : the official journal of the International Society for Endovascular Surgery*. 4:169-173.

Ocana, E., J.C. Bohorquez, J. Perez-Requena, J.A. Brieva, and C. Rodriguez. 2003. Characterisation of T and B lymphocytes infiltrating abdominal aortic aneurysms. *Atherosclerosis*. 170:39-48.

Oukka, M. 2008. Th17 cells in immunity and autoimmunity. *Annals of the rheumatic diseases*. 67 Suppl 3:iii26-29.

Oya, K., N. Sakamoto, T. Ohashi, and M. Sato. 2011. Combined stimulation with cyclic stretching and hypoxia increases production of matrix metalloproteinase-9 and cytokines by macrophages. *Biochemical and biophysical research communications*. 412:678-682.

Pajulo, O.T., K.J. Pulkki, M.S. Alanen, M.S. Reunanen, K.K. Lertola, A.I. Mattila-Vuori, and J.A. Viljanto. 1999. Correlation between interleukin-6 and matrix metalloproteinase-9 in early wound healing in children. *Wound repair and regeneration : official publication of the Wound Healing Society [and] the European Tissue Repair Society*. 7:453-457.

Pearce, W.H., and A.E. Koch. 1996. Cellular components and features of immune response in abdominal aortic aneurysms. *Annals of the New York Academy of Sciences*. 800:175-185.

Pearce, W.H., and V.P. Shively. 2006. Abdominal aortic aneurysm as a complex multifactorial disease: interactions of polymorphisms of inflammatory genes,

features of autoimmunity, and current status of MMPs. *Ann N Y Acad Sci*. 1085:117-132.

Pereira, L., S.Y. Lee, B. Gayraud, K. Andrikopoulos, S.D. Shapiro, T. Bunton, N.J. Biery, H.C. Dietz, L.Y. Sakai, and F. Ramirez. 1999. Pathogenetic sequence for aneurysm revealed in mice underexpressing fibrillin-1. *Proceedings of the National Academy of Sciences of the United States of America*. 96:3819-3823.

Petersen, E., F. Wagberg, and K.A. Angquist. 2002. Proteolysis of the abdominal aortic aneurysm wall and the association with rupture. *European journal of vascular and endovascular surgery : the official journal of the European Society for Vascular Surgery*. 23:153-157.

Pietrowski, E., B. Bender, J. Huppert, R. White, H.J. Luhmann, and C.R. Kuhlmann. 2011. Pro-inflammatory effects of interleukin-17A on vascular smooth muscle cells involve NAD(P)H- oxidase derived reactive oxygen species. *Journal of vascular research*. 48:52-58.

Radonic, T., P. de Witte, M. Groenink, V. de Waard, R. Lutter, M. van Eijk, M. Jansen, J. Timmermans, M. Kempers, A.J. Scholte, Y. Hilhorst-Hofstee, M.P. van den Berg, J.P. van Tintelen, G. Pals, M.J. Baars, B.J. Mulder, and A.H. Zwinderman. 2012. Inflammation aggravates disease severity in Marfan syndrome patients. *PloS one*. 7:e32963.

Rajagopalan, S., X.P. Meng, S. Ramasamy, D.G. Harrison, and Z.S. Galis. 1996. Reactive oxygen species produced by macrophage-derived foam cells regulate the activity of vascular matrix metalloproteinases in vitro. Implications for

atherosclerotic plaque stability. *The Journal of clinical investigation*. 98:2572-2579.

Recinos, A., 3rd, W.S. LeJeune, H. Sun, C.Y. Lee, B.C. Tieu, M. Lu, T. Hou, I. Boldogh, R.G. Tilton, and A.R. Brasier. 2007. Angiotensin II induces IL-6 expression and the Jak-STAT3 pathway in aortic adventitia of LDL receptor-deficient mice. *Atherosclerosis*. 194:125-133.

Rizas, K.D., N. Ippagunta, and M.D. Tilson, 3rd. 2009. Immune cells and molecular mediators in the pathogenesis of the abdominal aortic aneurysm. *Cardiol Rev*. 17:201-210.

Saraff, K., F. Babamusta, L.A. Cassis, and A. Daugherty. 2003. Aortic dissection precedes formation of aneurysms and atherosclerosis in angiotensin II-infused, apolipoprotein E-deficient mice. *Arteriosclerosis, thrombosis, and vascular biology*. 23:1621-1626.

Schonbeck, U., G.K. Sukhova, N. Gerdes, and P. Libby. 2002. T(H)2 predominant immune responses prevail in human abdominal aortic aneurysm. *Am J Pathol*. 161:499-506.

Schrader, L.I., D.A. Kinzenbaw, A.W. Johnson, F.M. Faraci, and S.P. Didion. 2007. IL-6 deficiency protects against angiotensin II induced endothelial dysfunction and hypertrophy. *Arteriosclerosis, thrombosis, and vascular biology*. 27:2576-2581.

Schuett, H., M. Luchtefeld, C. Grothusen, K. Grote, and B. Schieffer. 2009. How much is too much? Interleukin-6 and its signalling in atherosclerosis. *Thrombosis and haemostasis*. 102:215-222.

Segura, A.M., R.E. Luna, K. Horiba, W.G. Stetler-Stevenson, H.A. McAllister, Jr., J.T. Willerson, and V.J. Ferrans. 1998. Immunohistochemistry of matrix metalloproteinases and their inhibitors in thoracic aortic aneurysms and aortic valves of patients with Marfan's syndrome. *Circulation*. 98:II331-337; discussion II337-338.

Senchenkova, E.Y., J. Russell, E. Kurmaeva, D. Ostanin, and D.N. Granger. 2011. Role of T lymphocytes in angiotensin II-mediated microvascular thrombosis. *Hypertension*. 58:959-965.

Shahrara, S., S.R. Pickens, A. Dorfleutner, and R.M. Pope. 2009. IL-17 induces monocyte migration in rheumatoid arthritis. *J Immunol*. 182:3884-3891.

Shahrara, S., S.R. Pickens, A.M. Mandelin, 2nd, W.J. Karpus, Q. Huang, J.K. Kolls, and R.M. Pope. 2010. IL-17-mediated monocyte migration occurs partially through CC chemokine ligand 2/monocyte chemoattractant protein-1 induction. *J Immunol*. 184:4479-4487.

Smith, E., K.M. Prasad, M. Butcher, A. Dobrian, J.K. Kolls, K. Ley, and E. Galkina. 2010. Blockade of interleukin-17A results in reduced atherosclerosis in apolipoprotein E-deficient mice. *Circulation*. 121:1746-1755.

Sprague, A.H., and R.A. Khalil. 2009. Inflammatory cytokines in vascular dysfunction and vascular disease. *Biochemical pharmacology*. 78:539-552.

Sugiyama, F., S. Haraoka, T. Watanabe, N. Shiota, K. Taniguchi, Y. Ueno, K. Tanimoto, K. Murakami, A. Fukamizu, and K. Yagami. 1997. Acceleration of atherosclerotic lesions in transgenic mice with hypertension by the activated

renin-angiotensin system. *Laboratory investigation; a journal of technical methods and pathology*. 76:835-842.

Sun, J., T. Shilagard, B. Bell, M. Motamedi, and G. Vargas. 2004. In vivo multimodal nonlinear optical imaging of mucosal tissue. *Optics express*. 12:2478-2486.

Tieu, B.C., X. Ju, C. Lee, H. Sun, W. Lejeune, A. Recinos, 3rd, A.R. Brasier, and R.G. Tilton. 2010. Aortic Adventitial Fibroblasts Participate in Angiotensin-Induced Vascular Wall Inflammation and Remodeling. *J Vasc Res*. 48:261-272.

Tieu, B.C., C. Lee, H. Sun, W. Lejeune, A. Recinos, 3rd, X. Ju, H. Spratt, D.C. Guo, D. Milewicz, R.G. Tilton, and A.R. Brasier. 2009. An adventitial IL-6/MCP1 amplification loop accelerates macrophage-mediated vascular inflammation leading to aortic dissection in mice. *J Clin Invest*. 119:3637-3651.

Tilson, M.D., C. Fu, S.X. Xia, D. Syn, Y. Yoon, and T. McCaffrey. 2000. Expression of molecular messages for angiogenesis by fibroblasts from aneurysmal abdominal aorta versus dermal fibroblasts. *Int J Surg Investig*. 1:453-457.

Uchida, H.A., F. Kristo, D.L. Rateri, H. Lu, R. Charnigo, L.A. Cassis, and A. Daugherty. 2010. Total lymphocyte deficiency attenuates AngII-induced atherosclerosis in males but not abdominal aortic aneurysms in apoE deficient mice. *Atherosclerosis*. 211:399-403.

van Es, T., G.H. van Puijvelde, O.H. Ramos, F.M. Segers, L.A. Joosten, W.B. van den Berg, I.M. Michon, P. de Vos, T.J. van Berkel, and J. Kuiper. 2009. Attenuated atherosclerosis upon IL-17R signaling disruption in LDLr deficient mice. *Biochemical and biophysical research communications*. 388:261-265.

Wang, M., D. Zhao, G. Spinetti, J. Zhang, L.Q. Jiang, G. Pintus, R. Monticone, and E.G. Lakatta. 2006. Matrix metalloproteinase 2 activation of transforming growth factor-beta1 (TGF-beta1) and TGF-beta1-type II receptor signaling within the aged arterial wall. *Arteriosclerosis, thrombosis, and vascular biology*. 26:1503-1509.

Wi, J.H., J.S. Moon, M.G. Choi, J.O. Kim, J.H. Do, J.K. Ryu, K.N. Shim, K.J. Lee, B.I. Jang, and H.J. Chun. 2009. Bowel preparation for capsule endoscopy: a prospective randomized multicenter study. *Gut and liver*. 3:180-185.

Williams, A., S. Davies, A.G. Stuart, D.G. Wilson, and A.G. Fraser. 2008. Medical treatment of Marfan syndrome: a time for change. *Heart*. 94:414-421.

Xie, T.X., D. Wei, M. Liu, A.C. Gao, F. Ali-Osman, R. Sawaya, and S. Huang. 2004. Stat3 activation regulates the expression of matrix metalloproteinase-2 and tumor invasion and metastasis. *Oncogene*. 23:3550-3560.

Xiong, W., R.A. Knispel, H.C. Dietz, F. Ramirez, and B.T. Baxter. 2008. Doxycycline delays aneurysm rupture in a mouse model of Marfan syndrome. *Journal of vascular surgery : official publication, the Society for Vascular Surgery [and] International Society for Cardiovascular Surgery, North American Chapter*. 47:166-172; discussion 172.

Xiong, W., T. Meisinger, R. Knispel, J.M. Worth, and B.T. Baxter. 2012. MMP-2 Regulates Erk1/2 Phosphorylation and Aortic Dilatation in Marfan Syndrome. *Circulation research*. 110:e92-e101.

Yang, H.H., J.M. Kim, E. Chum, C. van Breemen, and A.W. Chung. 2010. Effectiveness of combination of losartan potassium and doxycycline versus single-drug treatments in the secondary prevention of thoracic aortic aneurysm in Marfan syndrome. *The Journal of thoracic and cardiovascular surgery*. 140:305-312 e302.

Zhao, L., M.P. Moos, R. Grabner, F. Pedrono, J. Fan, B. Kaiser, N. John, S. Schmidt, R. Spanbroek, K. Lotzer, L. Huang, J. Cui, D.J. Rader, J.F. Evans, A.J. Habenicht, and C.D. Funk. 2004. The 5-lipoxygenase pathway promotes pathogenesis of hyperlipidemia-dependent aortic aneurysm. *Nat Med*. 10:966-973.

Zipfel, W.R., R.M. Williams, R. Christie, A.Y. Nikitin, B.T. Hyman, and W.W. Webb. 2003. Live tissue intrinsic emission microscopy using multiphoton-excited native fluorescence and second harmonic generation. *Proceedings of the National Academy of Sciences of the United States of America*. 100:7075-7080.

VITA

Xiaoxi Ju

Ms. Xiaoxi Ju was born in Guangzhou, China on November 1st, 1984. In 2006, she graduates with Dean's Honor from Xiamen University, majoring in biological sciences. In 2009, she joined the vascular inflammation research group at UTMB under the guidance of professors Allan R. Brasier, MD and Ronald G. Tilton, PhD., where she performed dissertation research on several projects. During her doctoral studies, she has been co-authored on 6 papers, including 2 first-authored research articles and one book chapter.

PULICATIONS:

Ju X, Lee C, Sun H, LeJeune W, Recinos A, III, Ju X, Spratt H, Guo DC, Milewicz D, Tilton RG, Brasier AR. 2012. IL-6 mediates aortic inflammation and dissections induced by angiotensin II via the Th17 lymphocyte-IL17 axis in C57BL/6 Mice. Manuscript submitted to *Arteriosclerosis, Thrombosis, and Vascular Biology.*

Ju X, Sun H, Lejeune W, Vargas G, Recinos A 3rd, Brasier AR, Tilton RG. 2012. IL-6 regulates vascular inflammation and MMP-mediated ECM degeneration in aortic aneurysms in mice with Marfan Syndrome. Manuscript submitted to *Arteriosclerosis, Thrombosis, and Vascular Biology.*

Ju X, Tilton RG, Brasier AR. Multifaceted role of Angiotensin II in vascular inflammation and aortic aneurysmal disease (Book chapter). 2011. *Etiology, Pathogenesis and Pathophysiology of Aortic Aneurysms and Aneurysm Rupture*. ISBN 978-953-307-523-5.

Ray S, Ju X, Sun H, Finnerty CC, Herndon DH, Brasier AR. 2012. IL-6 Trans-signaling STAT3 pathway mediates ECM and cellular proliferation in fibroblasts from hypertrophic scar. Manuscript submitted to *Journal of investigative dermatology*.

Tieu BC, Ju X, Lee C, Sun H, Lejeune W, Recinos A III, Brasier AR, Tilton RG. Aortic Adventitial Fibroblasts Participate in Angiotensin-Induced Vascular Wall Inflammation and Remodeling. *J Vasc Res*. 2010; 23;48(3):261-272.

Tieu BC, Lee C, Sun H, LeJeune W, Recinos A, III, Ju X, Spratt H, Guo DC, Milewicz D, Tilton RG, Brasier AR. An adventitial IL-6/MCP1 amplification loop accelerates macrophage-mediated vascular inflammation leading to aortic dissection in mice. *J Clin Invest*. 2009; 119(12):3637-3651.

Abstracts:
Brasier AR, Tieu BC, Ju X, Recinos A, III, Guo DC, Milewicz D and Tilton RG. 2009. Ang II infusion and vascular inflammation through IL-6 signaling in a mouse model. Abstract for platform presentation, Aortic Disease Summit. Baltimore, MD.

Alfson D, Ju X, Recinos A III, Brasier AR. 2010. Construction of an inducible, fibroblast-specific NF- κ B/RelA knockout mouse model by Cre/lox-mediated gene inactivation for the study of vascular inflammation. Medical Student Research Conference. Galveston, TX.

Rodriguez P, Ju X, Recinos A, III, Brasier AR. 2010. Role of IL-6 and TGF-β in a mouse model of Angiotensin II-induced aortic aneurysms. SURP Research Conference. Galveston, TX. Best Poster Award.